

1                   **ON THE VLASOV-MAXWELL SYSTEM WITH A STRONG**  
2   **MAGNETIC FIELD\***

3                   FRANCIS FILBET<sup>†</sup>, TAO XIONG<sup>‡</sup>, AND ERIC SONNENDRÜCKER<sup>§</sup>

4           **Abstract.** This paper establishes the long time asymptotic limit of the  $2d \times 3d$  Vlasov-Maxwell  
5 system with a strong external magnetic field. Hence, a guiding center approximation is obtained in  
6 the two dimensional case with a self-consistent electromagnetic field given by Poisson type equations.  
7 Then, we perform several numerical experiments with high order approximation of the asymptotic  
8 model, which provide a solid validation of the method and illustrate the effect of the self-consistent  
9 magnetic field on the current density.

10    **Key words.** Asymptotic limit; High order scheme; Vlasov-Maxwell system; Finite difference  
11 methods.

12    **AMS subject classifications.** 65M20, 35Q83, 78A25

13    **1. Introduction.** We consider a plasma confined by a strong external magnetic  
14 field, hence the charged gas evolves under its self-consistent electromagnetic field and  
15 the confining magnetic field. This configuration is typical of a tokamak plasma [3, 30],  
16 where the magnetic field is used to confine particles inside the core of the device.

17    We assume that on the time scale we consider, collisions can be neglected both  
18 for ions and electrons, hence collective effects are dominant and the plasma is entirely  
19 modelled with kinetic transport equations, where the unknown is the number density  
20 of particles  $f \equiv f(t, \mathbf{x}, \mathbf{v})$  depending on time  $t \geq 0$ , position  $\mathbf{x} \in D \subset \mathbb{R}^3$  and velocity  
21  $\mathbf{v} \in \mathbb{R}^3$ .

22    Such a kinetic model provides an appropriate description of turbulent transport  
23 in a fairly general context, but it requires to solve a six dimensional problem which  
24 leads to a huge computational cost. To reduce the cost of numerical simulations, it  
25 is classical to derive asymptotic models with a smaller number of variables than the  
26 kinetic description. Large magnetic fields usually lead to the so-called drift-kinetic  
27 limit [1, 8, 28, 27] and we refer to [4, 7, 19, 20, 14, 21] for recent mathematical results  
28 on this topic. In this regime, due to the large applied magnetic field, particles are  
29 confined along the magnetic field lines and their period of rotation around these lines  
30 (called the cyclotron period) becomes small. It corresponds to the finite Larmor  
31 radius scaling for the Vlasov-Poisson equation, which was introduced by Frénod and  
32 Sonnendrücker in the mathematical literature [19, 20]. The two-dimensional version  
33 of the system (obtained when one restricts to the perpendicular dynamics) and the  
34 large magnetic field limit were studied in [14] and more recently in [4, 31, 24]. We also  
35 refer to the recent work [26] of Hauray and Nouri, dealing with the well-posedness  
36 theory with a diffusive version of a related two dimensional system. A version of the  
37 full three dimensional system describing ions with massless electrons was studied by

---

\*Submitted to the editors DATE.

**Funding:** This work was funded by the Fog Research Institute under contract no. FRI-454.

<sup>†</sup>Université de Toulouse III & IUF, UMR5219, Institut de Mathématiques de Toulouse, 118, route de Narbonne, F-31062 Toulouse cedex, FRANCE ([francis.filbet@math.univ-toulouse.fr](mailto:francis.filbet@math.univ-toulouse.fr)).

<sup>‡</sup>School of Mathematical Sciences, Fujian Provincial Key Laboratory of Math. Mod. & HPSC, Xiamen University, Xiamen, Fujian, P.R. China, 361005 and Université de Toulouse III, UMR5219, Institut de Mathématiques de Toulouse, 118, route de Narbonne, F-31062 Toulouse cedex, FRANCE ([tao.xiong@math.univ-toulouse.fr](mailto:tao.xiong@math.univ-toulouse.fr)).

<sup>§</sup>Max Planck Institute for Plasma Physics & Mathematics Center, TU Munich, Boltzmannstr. 2, 85748 Garching, GERMANY ([eric.sonnendruecker@ipp.mpg.de](mailto:eric.sonnendruecker@ipp.mpg.de)).

38 Han-Kwan in [23, 25].

39 Here we formally derive a new asymptotic model under both assumptions of large  
 40 magnetic field and large time asymptotic limit for the two dimensional in space and  
 41 three dimensional in velocity ( $2d \times 3d$ ) Vlasov-Maxwell system. An analogous problem  
 42 for the Vlasov-Poisson system has already been carefully studied by F. Golse and L.  
 43 Saint-Raymond in two dimension [21, 32, 22], and recently by P. Degond and F. Filbet  
 44 in three dimension [12]. In this paper, we will follow [12] to introduce some main char-  
 45 acteristic scales to rewrite the Vlasov-Maxwell system in a dimensionless form, and  
 46 reformulate the Maxwell equations by defining two potential functions correspond-  
 47 ing to the self-consistent electromagnetic field. We consider a small cyclotron period,  
 48 where the plasma frequency is relatively small as compared to the cyclotron frequency,  
 49 and study the long time behavior of the plasma. Assuming a constant strong external  
 50 magnetic field and that the distribution function is homogeneous along the external  
 51 magnetic field, an asymptotic kinetic model can be derived by performing Hilbert  
 52 expansions and comparing the first three leading order terms in terms of the small cy-  
 53 clotron period, thanks to passing in the cylindrical coordinates. The new asymptotic  
 54 model is composed of two two dimensional transport equations for the distribution  
 55 functions of ions and electrons respectively, averaging in the velocity plane orthogonal  
 56 to the external magnetic field, and a Poisson's equation for determining the electric  
 57 potential as well as an elliptic equation for the magnetic potential. It is incompressible  
 58 with a divergence free transport velocity and shares several good features with the  
 59 original Vlasov-Maxwell system, such as conservation of moments in velocity, total  
 60 energy, as well as the  $L^p$  norm and physical bounds. The existence of weak solutions  
 61 for the asymptotic model can also be obtained by following the lines of existence of  
 62 weak solutions for the Vlasov-Poisson system [2, 13], with some  $L^p$  estimates on the  
 63 charge density and current. Moreover, as the Mach number goes to 0 in the self-  
 64 consistent magnetic field, we can recover the two dimensional guiding-center model,  
 65 which is an asymptotic model for the Vlasov-Poisson system under the same scalings  
 66 [21, 36, 29].

67 A high order numerical scheme will be applied to solve the new asymptotic model,  
 68 which is an extension of the one developed by C. Yang and F. Filbet [36] for the two  
 69 dimensional guiding center model. Some other recent numerical methods for the  
 70 Vlasov-Poisson system or the two dimensional guiding-center model can be referred  
 71 to [15, 34, 10, 9, 18, 16, 35] and reference therein. Here a Hermite weighted essen-  
 72 tially non-oscillatory (HWENO) scheme is adopted for the two dimensional transport  
 73 equation, as well as the fast Fourier transform (FFT) or a 5-point central difference  
 74 scheme for the Poisson equation of the electric potential and the 5-point central dif-  
 75 ference scheme for the elliptic equation of the magnetic potential. We will compare  
 76 the asymptotic kinetic model with the two dimensional guiding-center model. With  
 77 some special initial datum as designed in the numerical examples, we will show that  
 78 under these settings, the two dimensional guiding-center model stays steady or nearly  
 79 steady, while the asymptotic model can create some instabilities with a small initial  
 80 nonzero current for the self-magnetic field. These instabilities are similar to some  
 81 classical instabilities, such as Kelvin-Helmholtz instability [18], diocotron instability  
 82 [36] for the two dimensional guiding-center model with some other perturbed initial  
 83 conditions, which can validate some good properties of our new asymptotic model.

84 The rest of the paper is organized as follows. In Section 2, the dimensionless  
 85 Vlasov-Maxwell system under some characteristic scales and the derivation of an  
 86 asymptotic model will be presented. The verification of preservation for some good  
 87 features as well as the existence of weak solutions for the asymptotic model will also

88 be given. The numerical scheme will be briefly described in Section 3 and followed  
 89 by some numerical examples in Section 4. Conclusions and our future work are in  
 90 Section 5.

91 **2. Mathematical modeling.** In this paper, we start from the Vlasov equation  
 92 for each species of ions and electrons,

$$93 \quad (1) \quad \partial_t f_s + \mathbf{v} \cdot \nabla_{\mathbf{x}} f_s + \frac{q_s}{m_s} \left( \mathbf{E} + \mathbf{v} \times (\mathbf{B} + \mathbf{B}_{ext}) \right) \cdot \nabla_{\mathbf{v}} f_s = 0, \quad s = i, e,$$

94 where  $f_s \equiv f_s(t, \mathbf{x}, \mathbf{v})$  is the distribution function,  $m_s$  and  $q_s$  are the mass and charge,  
 95 with  $s = i, e$  for the ions and electrons respectively. Here we assume that the ions  
 96 have an opposite charge to the electrons  $q_i = e = -q_e$  and consider a given large  
 97 magnetic field  $\mathbf{B}_{ext}$ , as well as self-consistent electromagnetic fields  $\mathbf{E}$  and  $\mathbf{B}$ , which  
 98 satisfy the Maxwell equations

$$99 \quad (2) \quad \begin{cases} \nabla_{\mathbf{x}} \times \mathbf{E} = -\partial_t \mathbf{B}, \\ \nabla_{\mathbf{x}} \times \mathbf{B} = \frac{1}{c^2} \partial_t \mathbf{E} + \mu_0 \mathbf{J}, \\ \nabla_{\mathbf{x}} \cdot \mathbf{E} = \frac{\rho}{\varepsilon_0}, \\ \nabla_{\mathbf{x}} \cdot \mathbf{B} = 0, \end{cases}$$

100 where  $c$  is the speed of light,  $\mu_0$  is the vacuum permeability,  $\varepsilon_0$  is the vacuum per-  
 101 mittivity and  $\mu_0 \varepsilon_0 = 1/c^2$ . The density  $n_s$ , average velocity  $\mathbf{u}_s$  are related to the  
 102 distribution function  $f_s$  by

$$103 \quad n_s = \int_{\mathbb{R}^3} f_s d\mathbf{v}, \quad n_s \mathbf{u}_s = \int_{\mathbb{R}^3} f_s \mathbf{v} d\mathbf{v},$$

104 hence we define the total charge density  $\rho$  and total current density  $\mathbf{J}$  as  $\rho =$   
 105  $e (n_i - n_e)$  and  $\mathbf{J} = e (n_i \mathbf{u}_i - n_e \mathbf{u}_e)$ .

106 **2.1. Rescaling of the Vlasov-Maxwell system.** In the following we will de-  
 107 rive an appropriate dimensionless scaling for (1) and (2) by introducing a set of  
 108 characteristic scales.

109 We assume that the plasma is such that the characteristic density and temperature  
 110 of ions and electrons are of the same order, that is,

$$111 \quad (3) \quad \bar{n} := \bar{n}_i = \bar{n}_e, \quad \bar{T} := \bar{T}_i = \bar{T}_e.$$

We choose to perform a scaling with respect to the ions. On the one hand, we set the  
 characteristic velocity scale  $\bar{v}$  as the thermal velocity corresponding to ions,

$$\bar{v} := \left( \frac{\kappa_B \bar{T}}{m_i} \right)^{1/2},$$

112 where  $\kappa_B$  is the Boltzmann constant. Then we define the characteristic length scale  
 113 of  $\bar{x}$  given by the Debye length, which is the same for ions and electrons

$$114 \quad \bar{x} := \lambda_D = \left( \frac{\varepsilon_0 \kappa_B \bar{T}}{\bar{n} e^2} \right)^{1/2}.$$

115 It allows to define a first time scale corresponding to the plasma frequency of ions  
 116  $\omega_p := \bar{v}/\bar{x}$ .

Finally, the characteristic magnitude of the electric field  $\mathbf{E}$  can be expressed from  $\bar{n}$  and  $\bar{x}$  by

$$\bar{E} := \frac{e\bar{n}\bar{x}}{\varepsilon_0},$$

117 hence the characteristic magnitude of the self-consistent magnetic field  $\mathbf{B}$ , which is  
 118 denoted by  $\bar{B}$ , is related to the scale of the electric field by  $\bar{E} = \bar{v}\bar{B}$ .

On the other hand, by denoting  $\bar{B}_{ext}$  the characteristic magnitude of the given magnetic field  $\mathbf{B}_{ext}$ , we define the cyclotron frequency corresponding to ions by

$$\omega_c := \frac{e\bar{B}_{ext}}{m_i}$$

119 and  $\omega_c^{-1}$  corresponds to a second time scale.

120 With the above introduced scales, we define the scaled variables as

$$121 \quad \mathbf{v}' = \frac{\mathbf{v}}{\bar{v}}, \quad \mathbf{x}' = \frac{\mathbf{x}}{\bar{x}}, \quad t' = \frac{t}{\bar{t}},$$

122 and the electromagnetic field as

$$123 \quad \mathbf{E}'(t', \mathbf{x}') = \frac{\mathbf{E}(t, \mathbf{x})}{\bar{E}}, \quad \mathbf{B}(t', \mathbf{x}') = \frac{\mathbf{B}(t, \mathbf{x})}{\bar{B}}, \quad \mathbf{B}'_{ext}(t', \mathbf{x}') = \frac{\mathbf{B}_{ext}(t, \mathbf{x})}{\bar{B}_{ext}}.$$

Furthermore, for each species, we define the characteristic velocity and subsequently, by letting  $\bar{f} = \bar{n}/\bar{v}^3$ ,

$$f'_s(t', \mathbf{x}', \mathbf{v}') = \frac{f_s(t, \mathbf{x}, \mathbf{v})}{\bar{f}}, \quad s = i, e.$$

124 Inserting all these new variables into (1), dividing by  $\omega_p$  and dropping the primes for  
 125 clarity, we obtain the following dimensionless Vlasov equation

$$126 \quad (4) \quad \begin{cases} \frac{1}{\omega_p \bar{t}} \partial_t f_i + \mathbf{v} \cdot \nabla_{\mathbf{x}} f_i + \left( \mathbf{E} + \mathbf{v} \times \mathbf{B} + \frac{\omega_c}{\omega_p} \mathbf{v} \times \mathbf{B}_{ext} \right) \cdot \nabla_{\mathbf{v}} f_i = 0, \\ \frac{1}{\omega_p \bar{t}} \partial_t f_e + \mathbf{v} \cdot \nabla_{\mathbf{x}} f_e - \frac{m_i}{m_e} \left( \mathbf{E} + \mathbf{v} \times \mathbf{B} + \frac{\omega_c}{\omega_p} \mathbf{v} \times \mathbf{B}_{ext} \right) \cdot \nabla_{\mathbf{v}} f_e = 0, \end{cases}$$

127 while the dimensionless Maxwell equations (2) are scaled according to the plasma  
 128 frequency of ions,

$$129 \quad (5) \quad \begin{cases} \nabla_{\mathbf{x}} \times \mathbf{E} = -\frac{1}{\omega_p \bar{t}} \partial_t \mathbf{B}, \\ \nabla_{\mathbf{x}} \times \mathbf{B} = \text{Ma}^2 \left( \frac{1}{\omega_p \bar{t}} \partial_t \mathbf{E} + \mathbf{J} \right), \\ \nabla_{\mathbf{x}} \cdot \mathbf{E} = \rho, \\ \nabla_{\mathbf{x}} \cdot \mathbf{B} = 0, \end{cases}$$

130 where  $\text{Ma} = \bar{v}/c$  is the Mach number and

$$131 \quad (6) \quad \rho = n_i - n_e, \quad \mathbf{J} = n_i \mathbf{u}_i - n_e \mathbf{u}_e.$$

132 To consider an asymptotic limit, we introduce a dimensionless cyclotron period  
133 of ions

$$134 \quad \varepsilon := \frac{\omega_p}{\omega_c},$$

where  $\varepsilon$  is a small parameter and study the long time asymptotic, that is,  $\varepsilon = 1/(\omega_p \bar{t}) \ll 1$ . We also denote by  $\alpha$  the mass ratio between electrons and ions

$$\alpha := \frac{m_e}{m_i}.$$

135 Under these two scalings, the Vlasov equation (4) takes the form

$$136 \quad (7) \quad \begin{cases} \varepsilon \partial_t f_i + \mathbf{v} \cdot \nabla_{\mathbf{x}} f_i + \left( \mathbf{E} + \mathbf{v} \times \mathbf{B} + \frac{1}{\varepsilon} \mathbf{v} \times \mathbf{B}_{ext} \right) \cdot \nabla_{\mathbf{v}} f_i = 0, \\ \varepsilon \partial_t f_e + \mathbf{v} \cdot \nabla_{\mathbf{x}} f_e - \frac{1}{\alpha} \left( \mathbf{E} + \mathbf{v} \times \mathbf{B} + \frac{1}{\varepsilon} \mathbf{v} \times \mathbf{B}_{ext} \right) \cdot \nabla_{\mathbf{v}} f_e = 0 \end{cases}$$

137 and the Maxwell equations (5) are

$$138 \quad (8) \quad \begin{cases} \nabla_{\mathbf{x}} \times \mathbf{E} = -\varepsilon \partial_t \mathbf{B}, \\ \nabla_{\mathbf{x}} \times \mathbf{B} = \text{Ma}^2 (\varepsilon \partial_t \mathbf{E} + \mathbf{J}), \\ \nabla_{\mathbf{x}} \cdot \mathbf{E} = \rho, \\ \nabla_{\mathbf{x}} \cdot \mathbf{B} = 0, \end{cases}$$

139 with  $\rho$  and  $\mathbf{J}$  given by (6).

140 **2.2. Asymptotic limit of the Vlasov-Maxwell system.** To derive an asymptotic  
141 model from (7)-(8), let us set our assumptions

142 **ASSUMPTION 2.1.** Consider  $\Omega \subset \mathbb{R}^2$  and  $D = \Omega \times [0, L_z]$ , the external magnetic  
143 field only applies in the  $z$ -direction

$$144 \quad \mathbf{B}_{ext} = (0, 0, 1)^t.$$

145 For simplicity we consider here periodic boundary conditions in space for the distribution  
146 function and the electromagnetic field.

147 **ASSUMPTION 2.2.** The plasma is homogeneous in the direction parallel to the applied  
148 magnetic field. Hence, the distribution functions  $f_i$  and  $f_e$  do not depend on  
149  $z$ .

150 For any  $\mathbf{x} = (x, y, z)^t \in \mathbb{R}^3$ , we decompose it as  $\mathbf{x} = \mathbf{x}_{\perp} + \mathbf{x}_{\parallel}$  according to the  
151 orthogonal and parallel directions to the external magnetic field  $\mathbf{B}_{ext}$ , that is,  $\mathbf{x}_{\perp} =$   
152  $(x, y, 0)^t$  and  $\mathbf{x}_{\parallel} = (0, 0, z)$ . In the same manner, the velocity is  $\mathbf{v} = \mathbf{v}_{\perp} + \mathbf{v}_{\parallel} \in \mathbb{R}^3$   
153 with  $\mathbf{v}_{\perp} = (v_x, v_y, 0)^t$  and  $\mathbf{v}_{\parallel} = (0, 0, v_z)$ . Under these assumptions and notations,

154 the Vlasov equation (7) can be written in the following form,

$$155 \quad (9) \quad \begin{cases} \varepsilon \partial_t f_i + \mathbf{v} \cdot \nabla_{\mathbf{x}} f_i + (\mathbf{E} + \mathbf{v} \times \mathbf{B}) \cdot \nabla_{\mathbf{v}} f_i + \frac{\mathbf{v}^\perp}{\varepsilon} \cdot \nabla_{\mathbf{v}} f_i = 0, \\ \varepsilon \partial_t f_e + \mathbf{v} \cdot \nabla_{\mathbf{x}} f_e - \frac{1}{\alpha} (\mathbf{E} + \mathbf{v} \times \mathbf{B}) \cdot \nabla_{\mathbf{v}} f_e - \frac{\mathbf{v}^\perp}{\varepsilon \alpha} \cdot \nabla_{\mathbf{v}} f_e = 0, \end{cases}$$

156 where  $\mathbf{v}^\perp = (v_y, -v_x, 0)$  for any  $\mathbf{v} \in \mathbb{R}^3$ .

Now we reformulate the Maxwell equations using Assumption 2.2. Here and after, we will drop the subindex  $\mathbf{x}$  for spatial derivatives of macroscopic quantities which do not depend on  $\mathbf{v}$ , such as  $\mathbf{E}$  and  $\mathbf{B}$  and their related quantities, for clarity. On the one hand, from the divergence free condition of (8), we can write  $\mathbf{B} = \nabla_{\mathbf{x}} \times \mathbf{A}$ , where  $\mathbf{A}$  is a magnetic potential verifying the Coulomb's gauge

$$\nabla_{\mathbf{x}} \cdot \mathbf{A} = 0.$$

On the other hand, the electric field  $\mathbf{E}$  is split into a longitudinal part and a transversal part  $\mathbf{E} = \mathbf{E}_L + \mathbf{E}_T$ , with

$$\begin{cases} \nabla_{\mathbf{x}} \times \mathbf{E}_L = 0, \\ \nabla_{\mathbf{x}} \cdot \mathbf{E}_T = 0. \end{cases}$$

157 From (8) it is easy to see that  $\mathbf{E}_L = -\nabla_{\mathbf{x}} \Phi$ , where the electrical potential  $\Phi$  is a  
158 solution to the Poisson's equation,

$$159 \quad (10) \quad -\Delta_{\mathbf{x}} \Phi = \rho.$$

160 Then, from (8) we get that

$$161 \quad \nabla_{\mathbf{x}} \times \mathbf{E}_T = -\partial_t \mathbf{B} = -\varepsilon \nabla_{\mathbf{x}} \times (\partial_t \mathbf{A}),$$

162 hence using the uniqueness of the decomposition for given boundary conditions, we  
163 necessarily have, assuming periodic boundary conditions, that  $\mathbf{E}_T = -\varepsilon \partial_t \mathbf{A}$  and the  
164 electric field  $\mathbf{E}$  is given by

$$165 \quad (11) \quad \mathbf{E} = -\nabla_{\mathbf{x}} \Phi - \varepsilon \partial_t \mathbf{A}.$$

166 Furthermore, the second equation in (8) gives the equation satisfied by the potential  
167  $\mathbf{A}$ , that is,

$$168 \quad (12) \quad (\varepsilon \text{Ma})^2 \partial_{tt}^2 \mathbf{A} - \Delta_{\mathbf{x}} \mathbf{A} = \text{Ma}^2 (\mathbf{J} - \varepsilon \partial_t \nabla_{\mathbf{x}} \Phi).$$

169 Gathering (10)-(12), we finally have  $\mathbf{E} = -\nabla_{\mathbf{x}} \Phi - \varepsilon \partial_t \mathbf{A}$  and  $\mathbf{B} = \nabla_{\mathbf{x}} \times \mathbf{A}$ ,

$$170 \quad (13) \quad \begin{cases} (\varepsilon \text{Ma})^2 \partial_{tt}^2 \mathbf{A} - \Delta_{\mathbf{x}} \mathbf{A} = \text{Ma}^2 (\mathbf{J} - \varepsilon \partial_t \nabla_{\mathbf{x}} \Phi), \\ -\Delta_{\mathbf{x}} \Phi = \rho. \end{cases}$$

171 Now we remind the basic properties of the solution to (9) and (13)

PROPOSITION 2.3. *We consider that Assumptions 2.1 and 2.2 are verified and  $(f_i^\varepsilon, f_e^\varepsilon, \Phi^\varepsilon, \mathbf{A}^\varepsilon)_{\varepsilon>0}$  is a solution to (9) and (13). Then we have for all  $t \geq 0$ ,*

$$\|f_s^\varepsilon(t)\|_{L^p} = \|f_s^\varepsilon(0)\|_{L^p}, \quad s = i, e.$$

172 Moreover we define the total energy at time  $t \geq 0$ , as

$$173 \quad \mathcal{E}^\varepsilon(t) := \int_{\mathbb{T}^2 \times \mathbb{R}^3} [f_i^\varepsilon(t) + \alpha f_e^\varepsilon(t)] \frac{|\mathbf{v}|^2}{2} d\mathbf{x}_\perp d\mathbf{v}$$

$$174 \quad + \frac{1}{2} \int_{\mathbb{T}^2} \left[ |\nabla_{\mathbf{x}} \Phi|^2 + \varepsilon |\partial_t \mathbf{A}|^2 + \frac{1}{Ma^2} |\nabla_{\mathbf{x}} \times \mathbf{A}|^2 \right] d\mathbf{x}_\perp,$$

175

176 which is conserved for all time  $t \geq 0$ ,  $\mathcal{E}^\varepsilon(t) = \mathcal{E}^\varepsilon(0)$ .

177 We now derive the asymptotic limit of (9) and (13) by letting  $\varepsilon \rightarrow 0$ . We denote  
178 the solutions to the above equations (9) and (13) as  $(f_i^\varepsilon, f_e^\varepsilon, \mathbf{A}^\varepsilon, \Phi^\varepsilon)$ , and perform  
179 Hilbert expansions for  $s = i, e$

$$180 \quad (14) \quad \begin{cases} f_s^\varepsilon = f_{s,0} + \varepsilon f_{s,1} + \varepsilon^2 f_{s,2} + \dots, \\ \mathbf{A}^\varepsilon = \mathbf{A}_0 + \varepsilon \mathbf{A}_1 + \dots, \\ \Phi^\varepsilon = \Phi_0 + \varepsilon \Phi_1 + \dots, \end{cases}$$

correspondingly

$$\mathbf{E}^\varepsilon = \mathbf{E}_0 + \varepsilon \mathbf{E}_1 + \dots, \quad \mathbf{B}^\varepsilon = \mathbf{B}_0 + \varepsilon \mathbf{B}_1 + \dots.$$

181 We prove the following asymptotic limit

THEOREM 2.4 (Formal expansion). *Consider that Assumptions 2.1 and 2.2 are satisfied. Let  $(f_i^\varepsilon, f_e^\varepsilon, \mathbf{A}^\varepsilon, \Phi^\varepsilon)$  be a nonnegative solution to the Vlasov-Maxwell system (9) and (13) satisfying (14). Then, the leading term  $(f_{i,0}, f_{e,0}, \Phi_0, \mathbf{A}_0)$  is such that*

$$\begin{cases} \Phi_0 \equiv \Phi(t, \mathbf{x}), \\ \mathbf{A}_0 \equiv (0, 0, A(t, \mathbf{x}))^t. \end{cases}$$

Furthermore, we define  $(F_i, F_e)$  as

$$F_i(t, \mathbf{x}, p_z) = \frac{1}{2\pi} \int_{\mathbb{R}^2} f_{i,0}(t, \mathbf{x}, \mathbf{v}) dv_x dv_y,$$

$$F_e(t, \mathbf{x}, q_z) = \alpha^{-1} \frac{1}{2\pi} \int_{\mathbb{R}^2} f_{e,0}(t, \mathbf{x}, \mathbf{v}) dv_x dv_y$$

where  $p_z = v_z + A(t, \mathbf{x})$  and  $q_z = \alpha v_z - A(t, \mathbf{x})$ , and the two Hamiltonians

$$\mathcal{H}_i = \Phi + \frac{1}{2} (A - p_z)^2 \quad \text{and} \quad \mathcal{H}_e = \Phi - \frac{1}{2\alpha} (q_z + A)^2,$$

182 where  $(F_i, F_e, \Phi, A)$  is a solution to the following system

$$183 \quad (15) \quad \begin{cases} \partial_t F_i - \nabla_{\mathbf{x}}^\perp \mathcal{H}_i \cdot \nabla_{\mathbf{x}} F_i = 0, \\ \partial_t F_e - \nabla_{\mathbf{x}}^\perp \mathcal{H}_e \cdot \nabla_{\mathbf{x}} F_e = 0, \\ -\Delta_{\mathbf{x}} \Phi = \rho, \\ -\Delta_{\mathbf{x}} A + Ma^2 \left( n_i + \frac{n_e}{\alpha} \right) A = Ma^2 \mathcal{J}_z, \end{cases}$$

184 and the density  $n_i$  and  $n_e$  are given by

$$185 \quad (16) \quad n_s = \int_{\mathbb{R}} F_s(t, \mathbf{x}, r_z) dr_z, \quad s = i, e,$$

186 hence the charge density is  $\rho = n_i - n_e$  and the current density corresponds to

$$187 \quad (17) \quad \mathcal{J}_z = \int_{\mathbb{R}} r_z \left( F_i(t, \mathbf{x}, r_z) - \frac{1}{\alpha} F_e(t, \mathbf{x}, r_z) \right) dr_z,$$

188 where the Mach number  $Ma = \bar{v}/c$ .

189 **REMARK 2.5.** Observe that the drift velocity in (15) called  $\mathbf{E} \times \mathbf{B} = \nabla_{\mathbf{x}}^{\perp} \Phi$  is the  
190 same for the two species, since it does not depend on the charge of the particle.

191 *Proof.* We first start with the self-consistent electromagnetic fields, we can easily  
192 find from (13) that  $\mathbf{E}_0 = -\nabla_{\mathbf{x}} \Phi_0$  and  $\mathbf{B}_0 = \nabla_{\mathbf{x}} \times \mathbf{A}_0$  with

$$193 \quad (18) \quad \begin{cases} -\Delta_{\mathbf{x}} \Phi_0 = \rho_0, \\ -\Delta_{\mathbf{x}} \mathbf{A}_0 = Ma^2 \mathbf{J}_0, \end{cases}$$

194 and at the next order  $\mathbf{E}_1 = -\nabla_{\mathbf{x}} \Phi_1 - \partial_t \mathbf{A}_0$  and  $\mathbf{B}_1 = \nabla_{\mathbf{x}} \times \mathbf{A}_1$ , with

$$195 \quad (19) \quad \begin{cases} -\Delta_{\mathbf{x}} \Phi_1 = \rho_1, \\ -\Delta_{\mathbf{x}} \mathbf{A}_1 = Ma^2 (\mathbf{J}_1 - \partial_t \nabla_{\mathbf{x}} \Phi_0), \end{cases}$$

where for  $k = 0, 1$ ,

$$\rho_k = \int_{\mathbb{R}^3} [f_{i,k} - f_{e,k}] d\mathbf{v}, \quad \mathbf{J}_k = \int_{\mathbb{R}^3} \mathbf{v} [f_{i,k} - f_{e,k}] d\mathbf{v}.$$

196 Substituting the Hilbert expansions into (9), and comparing the orders of  $\varepsilon$ , such as  
197  $\varepsilon^{-1}, \varepsilon^0$  and  $\varepsilon$ , we obtain the following three equations for ions:

$$198 \quad (20) \quad \begin{cases} \mathbf{v}^{\perp} \cdot \nabla_{\mathbf{v}} f_{i,0} = 0, \\ \mathbf{v} \cdot \nabla_{\mathbf{x}} f_{i,0} + (\mathbf{E}_0 + \mathbf{v} \times \mathbf{B}_0) \cdot \nabla_{\mathbf{v}} f_{i,0} = -\mathbf{v}^{\perp} \cdot \nabla_{\mathbf{v}} f_{i,1}, \\ \partial_t f_{i,0} + \mathbf{v} \cdot \nabla_{\mathbf{x}} f_{i,1} + (\mathbf{E}_0 + \mathbf{v} \times \mathbf{B}_0) \cdot \nabla_{\mathbf{v}} f_{i,1} + (\mathbf{E}_1 + \mathbf{v} \times \mathbf{B}_1) \cdot \nabla_{\mathbf{v}} f_{i,0} \\ = -\mathbf{v}^{\perp} \cdot \nabla_{\mathbf{v}} f_{i,2} \end{cases}$$

199 and for electrons:

$$200 \quad (21) \quad \begin{cases} \mathbf{v}^{\perp} \cdot \nabla_{\mathbf{v}} f_{e,0} = 0, \\ \alpha \mathbf{v} \cdot \nabla_{\mathbf{x}} f_{e,0} - (\mathbf{E}_0 + \mathbf{v} \times \mathbf{B}_0) \cdot \nabla_{\mathbf{v}} f_{e,0} = \mathbf{v}^{\perp} \cdot \nabla_{\mathbf{v}} f_{e,1}, \\ \alpha (\partial_t f_{e,0} + \mathbf{v} \cdot \nabla_{\mathbf{x}} f_{e,1}) - (\mathbf{E}_0 + \mathbf{v} \times \mathbf{B}_0) \cdot \nabla_{\mathbf{v}} f_{e,1} - (\mathbf{E}_1 + \mathbf{v} \times \mathbf{B}_1) \cdot \nabla_{\mathbf{v}} f_{e,0} \\ = \mathbf{v}^{\perp} \cdot \nabla_{\mathbf{v}} f_{e,2}. \end{cases}$$

We now pass in cylindrical coordinates in velocity  $\mathbf{v} = \mathbf{v}_{\perp} + \mathbf{v}_{\parallel}$ , with

$$\mathbf{v}_{\perp} = \omega \mathbf{e}_{\omega},$$

201 where we have set  $\omega = |\mathbf{v}_\perp|$  and

$$202 \quad \mathbf{e}_\omega = \begin{pmatrix} \cos \theta \\ \sin \theta \\ 0 \end{pmatrix}, \quad \mathbf{e}_\theta = \begin{pmatrix} -\sin \theta \\ \cos \theta \\ 0 \end{pmatrix}.$$

203 Using these notations, we now derive the asymptotic limit according to the orders  
204 of  $\varepsilon$  in (20)-(21). First the leading order term in (20)-(21) written in cylindrical  
205 coordinates becomes

$$206 \quad -\partial_\theta f_{s,0} = 0, \quad s = i, e,$$

207 which means that  $f_{s,0}$  does not depend on  $\theta$ , hence from Assumption 2.2, it yields  
208 that  $f_{s,0} \equiv f_{s,0}(t, \mathbf{x}_\perp, \omega, v_z)$ .

209 As a consequence, the current density is such that

$$210 \quad (n_s \mathbf{u}_{s,0})_\perp := \int_{\mathbb{R}^3} \mathbf{v}_\perp f_{s,0} d\mathbf{v} = \int_{\mathbb{R}} \int_0^\infty f_{s,0} \left( \int_0^{2\pi} \mathbf{e}_\omega d\theta \right) \omega^2 d\omega dv_z = \mathbf{0},$$

which implies that only the third component of the total current density  $\mathbf{J}_0$  might  
be nonzero and therefore only the third component of  $\mathbf{A}_0$  in (18) might be nonzero,  
that is,  $\mathbf{A}_0 = (0, 0, A_0)$  is a solution to the Poisson's equation with the source term  
 $\mathbf{J}_0 = (0, 0, j_z)$

$$-\Delta_{\mathbf{x}} A_0 = \text{Ma}^2 j_z,$$

211 hence from  $\mathbf{B}_0 = \nabla_{\mathbf{x}} \times \mathbf{A}_0$ , it yields that  $\mathbf{B}_0 = \nabla_{\mathbf{x}}^\perp A_0$  and particularly  $B_{0,z} = 0$ .

212 Finally, since the electric field  $\mathbf{E}_0 = -\nabla_{\mathbf{x}} \Phi_0$  and from Assumption 2.2, we also  
213 have that  $E_{0,z} = 0$ .

214

215 Now we treat the zeroth order term in (20)-(21) and use the cylindrical coordinates  
216 in the velocity variable, it gives

$$217 \quad (22) \quad \partial_\theta f_{i,1} = \mathbf{e}_\omega \cdot \mathbf{G}_{i,0}, \quad \partial_\theta f_{e,1} = \mathbf{e}_\omega \cdot \mathbf{G}_{e,0},$$

218 with

$$219 \quad (23) \quad \begin{cases} \mathbf{G}_{i,0} = +(\omega \nabla_{\mathbf{x}} f_{i,0} - (\nabla_{\mathbf{x}} \Phi_0 - v_z \nabla_{\mathbf{x}} A_0) \partial_\omega f_{i,0} - \omega \nabla_{\mathbf{x}} A_0 \partial_{v_z} f_{i,0}), \\ \mathbf{G}_{e,0} = -(\alpha \omega \nabla_{\mathbf{x}} f_{e,0} + (\nabla_{\mathbf{x}} \Phi_0 - v_z \nabla_{\mathbf{x}} A_0) \partial_\omega f_{e,0} + \omega \nabla_{\mathbf{x}} A_0 \partial_{v_z} f_{e,0}). \end{cases}$$

First notice that  $\mathbf{G}_{e,0}$  and  $\mathbf{G}_{i,0}$  do not depend on  $\theta \in (0, 2\pi)$  since  $f_0$  does not depend  
on  $\theta$  and

$$\int_0^{2\pi} \mathbf{e}_\omega d\theta = \mathbf{0},$$

220 then the solvability condition of (22) is automatically satisfied and after integration  
221 in  $\theta$ , we obtain  $f_1$  as,

$$222 \quad (24) \quad \begin{cases} f_{i,1}(t, \mathbf{x}_\perp, \omega, \theta, v_z) = -\mathbf{e}_\theta \cdot \mathbf{G}_{i,0}(t, \mathbf{x}_\perp, \omega, v_z) + h_i(t, \mathbf{x}_\perp, \omega, v_z), \\ f_{e,1}(t, \mathbf{x}_\perp, \omega, \theta, v_z) = -\mathbf{e}_\theta \cdot \mathbf{G}_{e,0}(t, \mathbf{x}_\perp, \omega, v_z) + h_e(t, \mathbf{x}_\perp, \omega, v_z), \end{cases}$$

223 where  $h_i$  and  $h_e$  are arbitrary functions which do not depend on  $\theta$ .

Now we focus on the first order with respect to  $\varepsilon$  in (20)-(21). Similarly, from the periodic boundary condition in  $\theta \in (0, 2\pi)$ , we have the following solvability condition

$$\frac{1}{2\pi} \int_0^{2\pi} \partial_\theta f_{s,2} d\theta = 0, \quad s = i, e.$$

224 Therefore, we have

$$225 \quad (25) \quad \left\{ \begin{array}{l} \partial_t f_{i,0} + \frac{1}{2\pi} \int_0^{2\pi} \left( \mathbf{v} \cdot \nabla_{\mathbf{x}} f_{i,1} + (\mathbf{E}_0 + \mathbf{v} \times \mathbf{B}_0) \cdot \nabla_{\mathbf{v}} f_{i,1} \right. \\ \quad \left. + (\mathbf{E}_1 + \mathbf{v} \times \mathbf{B}_1) \cdot \nabla_{\mathbf{v}} f_{i,0} \right) d\theta = 0, \\ \alpha \partial_t f_{e,0} + \frac{1}{2\pi} \int_0^{2\pi} \left( \alpha \mathbf{v} \cdot \nabla_{\mathbf{x}} f_{e,1} - (\mathbf{E}_0 + \mathbf{v} \times \mathbf{B}_0) \cdot \nabla_{\mathbf{v}} f_{e,1} \right. \\ \quad \left. - (\mathbf{E}_1 + \mathbf{v} \times \mathbf{B}_1) \cdot \nabla_{\mathbf{v}} f_{e,0} \right) d\theta = 0. \end{array} \right.$$

226 Each integral term can be explicitly calculated by substituting  $f_{i,1}$  and  $f_{e,1}$  from (24).

227 On the one hand, observing that

$$228 \quad \left\{ \begin{array}{l} \partial_\omega f_{s,1} = -\mathbf{e}_\theta \cdot \partial_\omega \mathbf{G}_{s,0} + \partial_\omega h_s, \quad s = i, e, \\ \partial_\theta f_{s,1} = \mathbf{e}_\omega \cdot \mathbf{G}_{s,0}, \quad s = i, e, \end{array} \right.$$

229 it yields for  $s = i, e$ ,

$$230 \quad (26) \quad \frac{1}{2\pi} \int_0^{2\pi} \mathbf{v} \cdot \nabla_{\mathbf{x}} f_{s,1} d\theta = -\frac{\omega}{2} \nabla_{\mathbf{x}} \cdot \mathbf{G}_{s,0}^\perp.$$

231 On the other hand, the same kind of computation leads to for  $s = i, e$ ,

$$232 \quad (27) \quad \frac{1}{2\pi} \int_0^{2\pi} (\mathbf{E}_0 + \mathbf{v} \times \mathbf{B}_0) \cdot \nabla_{\mathbf{v}} f_{s,1} d\theta \\ 233 \quad = -\frac{1}{2} \left[ \frac{(\mathbf{E}_0 + v_z \nabla_{\mathbf{x}} A_0)}{\omega} \cdot \partial_\omega (\omega \mathbf{G}_{s,0}^\perp) - \omega \nabla_{\mathbf{x}} A_0 \cdot \partial_{v_z} \mathbf{G}_{s,0}^\perp \right]. \\ 234$$

235 Finally since  $f_{s,0}$  does not depend on  $\theta \in (0, 2\pi)$  and the electric field does not  
236 depend on  $z$ , the last term in (25) only gives

$$237 \quad (28) \quad \frac{1}{2\pi} \int_0^{2\pi} (\mathbf{E}_1 + \mathbf{v} \times \mathbf{B}_1) \cdot \nabla_{\mathbf{v}} f_{s,0} d\theta = -\partial_t A_0 \partial_{v_z} f_{s,0}, \quad s = i, e.$$

238 Gathering (26)-(28), and recalling that  $\mathbf{E}_0 = -\nabla_{\mathbf{x}} \Phi_0$ , we get for the distribution  
239 function  $f_{i,0}$ ,

$$240 \quad \partial_t f_{i,0} - \frac{\omega}{2} \nabla_{\mathbf{x}} \cdot \mathbf{G}_{i,0}^\perp + \frac{1}{2} \left( \frac{\nabla_{\mathbf{x}} (\Phi_0 - v_z A_0)}{\omega} \cdot \partial_\omega (\omega \mathbf{G}_{i,0}^\perp) + \omega \nabla_{\mathbf{x}} A_0 \cdot \partial_{v_z} \mathbf{G}_{i,0}^\perp \right) \\ 241 \\ 243 \quad - \partial_t A_0 \partial_{v_z} f_{i,0} = 0.$$

244 and for the distribution function  $f_{e,0}$ ,

$$245 \quad \alpha \left( \partial_t f_{e,0} - \frac{\omega}{2} \nabla_{\mathbf{x}} \cdot \mathbf{G}_{e,0}^\perp \right) - \frac{1}{2} \left( \frac{\nabla_{\mathbf{x}} (\Phi_0 - v_z A_0)}{\omega} \cdot \partial_\omega (\omega \mathbf{G}_{e,0}^\perp) + \omega \nabla_{\mathbf{x}} A_0 \cdot \partial_{v_z} \mathbf{G}_{e,0}^\perp \right)$$

$$246 \quad + \partial_t A_0 \partial_{v_z} f_{e,0} = 0.$$

249 Using the definition of  $\mathbf{G}_{s,0}$  for  $s = i, e$  in (23) and after some calculations, it finally  
250 yields that

$$(29) \quad \begin{cases} \partial_t f_{i,0} - \nabla_{\mathbf{x}}^\perp (\Phi_0 - v_z A_0) \cdot \nabla_{\mathbf{x}} f_{i,0} - (\nabla_{\mathbf{x}} \Phi_0 \cdot \nabla_{\mathbf{x}}^\perp A_0 + \partial_t A_0) \partial_{v_z} f_{i,0} = 0, \\ \alpha (\partial_t f_{e,0} - \nabla_{\mathbf{x}}^\perp (\Phi_0 - v_z A_0) \cdot \nabla_{\mathbf{x}} f_{e,0}) + (\nabla_{\mathbf{x}} \Phi_0 \cdot \nabla_{\mathbf{x}}^\perp A_0 + \partial_t A_0) \partial_{v_z} f_{e,0} = 0. \end{cases}$$

Observing that this equation does not explicitly depend on  $\omega$ , we define

$$F_{s,0}(t, \mathbf{x}_\perp, v_z) := \frac{1}{2\pi} \int_{\mathbb{R}^2} f_{s,0}(t, \mathbf{x}_\perp, \mathbf{v}) dv_x dv_y, \quad s = i, e.$$

252 Multiplying (29) by  $\omega$  and integrating with respect to  $\omega$ , we get

$$(30) \quad \begin{cases} \partial_t F_{i,0} - \nabla_{\mathbf{x}}^\perp (\Phi_0 - v_z A_0) \cdot \nabla_{\mathbf{x}} F_{i,0} - (\nabla_{\mathbf{x}} \Phi_0 \cdot \nabla_{\mathbf{x}}^\perp A_0 + \partial_t A_0) \partial_{v_z} F_{i,0} = 0, \\ \alpha (\partial_t F_{e,0} - \nabla_{\mathbf{x}}^\perp (\Phi_0 - v_z A_0) \cdot \nabla_{\mathbf{x}} F_{e,0}) + (\nabla_{\mathbf{x}} \Phi_0 \cdot \nabla_{\mathbf{x}}^\perp A_0 + \partial_t A_0) \partial_{v_z} F_{e,0} = 0. \end{cases}$$

This last equation can be reformulated to remove the time derivative of  $A_0$  in the velocity field. To this aim, we introduce a new variable for  $p_z = v_z + A_0(t, \mathbf{x})$  in  $F_{i,0}$  and  $q_z = \alpha v_z - A_0(t, \mathbf{x})$  in  $F_{e,0}$  and perform a change of variable in velocity

$$F_i(t, \mathbf{x}_\perp, p_z) = F_{i,0}(t, \mathbf{x}_\perp, v_z), \quad F_e(t, \mathbf{x}_\perp, q_z) = \alpha^{-1} F_{e,0}(t, \mathbf{x}_\perp, v_z).$$

From now on, we will use  $\Phi(t, \mathbf{x})$  and  $A(t, \mathbf{x})$  in short of  $\Phi_0(t, \mathbf{x})$  and  $A_0(t, \mathbf{x})$  respectively. Hence (30) now becomes

$$\begin{cases} \partial_t F_i - \nabla_{\mathbf{x}}^\perp \mathcal{H}_i \cdot \nabla_{\mathbf{x}} F_i = 0, \\ \partial_t F_e - \nabla_{\mathbf{x}}^\perp \mathcal{H}_e \cdot \nabla_{\mathbf{x}} F_e = 0, \end{cases}$$

with

$$\mathcal{H}_i = \Phi + \frac{1}{2} (A - p_z)^2 \quad \text{and} \quad \mathcal{H}_e = \Phi - \frac{1}{2\alpha} (A + q_z)^2,$$

where the charge density is always given by  $\rho = n_i - n_e$ , whereas the current density is now given by

$$j_z = \mathcal{J}_z - \left( n_i + \frac{n_e}{\alpha} \right) A,$$

254 where  $(n_i, n_e)$  and  $\mathcal{J}_z$  are respectively defined in (16) and (17). Finally, the potentials  
255  $(\Phi, A)$  are now solutions to

$$256 \quad \begin{cases} -\Delta_{\mathbf{x}} \Phi = \rho, \\ -\Delta_{\mathbf{x}} A + \text{Ma}^2 \left( n_i + \frac{n_e}{\alpha} \right) A = \text{Ma}^2 \mathcal{J}_z, \end{cases}$$

257 where  $\text{Ma} = \bar{v}/c$  is the Mach number. □

258 **2.3. Weak solutions for the asymptotic model.** First notice that the asymp-  
 259 totic model (15) is now two dimensional in space since we assume that the plasma is  
 260 homogeneous in the parallel direction to the external magnetic field and one dimen-  
 261 sional in moment since we have averaged in the orthogonal direction to the external  
 262 magnetic field.

263 To simplify the presentation, from now on  $\mathbf{x}$  represents the orthogonal part of  
 264  $\mathbf{x}_\perp = (x, y, 0)$  with  $(x, y) \in \Omega$ .

265 For the sake of simplicity in the analysis we have only considered periodic bound-  
 266 ary conditions in space, for  $\mathbf{x} \in \Omega := (0, L_x) \times (0, L_y)$ ,

$$(31) \quad \left\{ \begin{array}{l} \Phi(t, x + L_x, y) = \Phi(t, x, y), \quad \Phi(t, x, y + L_y) = \Phi(t, x, y), \\ A(t, x + L_x, y) = A(t, x, y), \quad A(t, x, y + L_y) = A(t, x, y), \\ F_i(t, x + L_x, y, p_z) = F_i(t, x, y, p_z), \quad F_i(t, x, y + L_y, p_z) = F_i(t, x, y, p_z), \quad p_z \in \mathbb{R}, \\ F_e(t, x + L_x, y, q_z) = F_e(t, x, y, q_z), \quad F_e(t, x, y + L_y, q_z) = F_e(t, x, y, q_z), \quad q_z \in \mathbb{R}. \end{array} \right.$$

268 But other kinds of boundary conditions may be treated for the asymptotic model as  
 269 homogeneous Dirichlet boundary conditions for the potential  $\Phi$  and  $A$

$$(32) \quad \Phi(t, \mathbf{x}) = 0, \quad A(t, \mathbf{x}) = 0, \quad \mathbf{x} \in \partial\Omega.$$

271 Then let us review the main features of the asymptotic model (15), which make  
 272 this mathematical model consistent with the initial Vlasov-Maxwell model (9) and  
 273 (13).

274 **PROPOSITION 2.6.** *Consider a solution to the asymptotic model (15) with the*  
 275 *boundary conditions (31), or (32), or a combination of both, then it satisfies*

- 276 • the flow remains incompressible ;
- 277 • for any  $m > 1$ , we have conservation of moments in velocity, for any time
- 278  $t \geq 0$ ,

$$(33) \quad \int_{\Omega \times \mathbb{R}} |r_z|^m F_s(t, \mathbf{x}, r_z) dr_z d\mathbf{x} = \int_{\Omega \times \mathbb{R}} |r_z|^m F_s(0, \mathbf{x}, r_z) dr_z d\mathbf{x}, \quad s = i, e;$$

- 280 • for any continuous function  $\phi : \mathbb{R} \mapsto \mathbb{R}$ , we have for any time  $t \geq 0$ ,

$$(34) \quad \int_{\Omega} \int_{\mathbb{R}} \phi(F_s(t, \mathbf{x}, r_z)) d\mathbf{x} dr_z = \int_{\Omega} \int_{\mathbb{R}} \phi(F_s(0, \mathbf{x}, r_z)) d\mathbf{x} dr_z, \quad s = i, e;$$

- 282 • the total energy defined by

$$(35) \quad \begin{aligned} \mathcal{E}(t) := & \int_{\mathbb{R}} \int_{\Omega} \frac{|r_z - A|^2}{2} F_i + \frac{|r_z + A|^2}{2\alpha} F_e d\mathbf{x} dr_z \\ & + \frac{1}{2} \int_{\Omega} |\nabla_{\mathbf{x}} \Phi|^2 + \frac{1}{Ma^2} |\nabla_{\mathbf{x}} A|^2 d\mathbf{x}, \end{aligned}$$

286 is conserved for all time  $t \geq 0$ .

*Proof.* The velocity field in (15) can be written as

$$\mathbf{U}_s(t, \mathbf{x}, p_z) = -\nabla_{\mathbf{x}}^\perp \mathcal{H}_s, \quad s = e, i,$$

287 hence  $\nabla_{\mathbf{x}} \cdot \mathbf{U}_s = 0$  is automatically satisfied and the flow is incompressible.

Then observing that the variable  $r_z \in \mathbb{R}$  only appears as a parameter in the equation, we prove the conservation of moments with respect to  $r_z$  : for any  $m > 1$  we have for  $s = i, e$ ,

$$\int_{\Omega \times \mathbb{R}} |r_z|^m F_s(t, \mathbf{x}, r_z) dr_z d\mathbf{x} = \int_{\Omega \times \mathbb{R}} |r_z|^m F(0, \mathbf{x}, r_z) dr_z d\mathbf{x}.$$

288 For a given smooth function  $\phi : \mathbb{R} \mapsto \mathbb{R}$  and  $s = i, e$ , if we multiply the first  
289 equation in (15) by  $\phi'(F_s)$ , it becomes

$$290 \quad \partial_t \phi(F_s) + \nabla_{\mathbf{x}} \cdot (\mathbf{U}_s \phi(F_s)) = 0.$$

291 Integrating the above equation in space  $\Omega$  we obtain

$$292 \quad \frac{\partial}{\partial t} \int_{\Omega} \phi(F_s) d\mathbf{x} = - \int_{\partial\Omega} \phi(F_s) \mathbf{U}_s(t, \mathbf{x}, r_z) \cdot \nu_{\mathbf{x}} d\sigma_{\mathbf{x}},$$

where  $\nu_{\mathbf{x}}$  is the outward normal to  $\partial\Omega$  at  $\mathbf{x}$ . Now for periodic boundary conditions (31), the right hand side is obviously zero, and for homogeneous Dirichlet boundary conditions (32), we observe that the tangential derivatives verify  $\nabla_{\mathbf{x}} \Phi \cdot \tau_{\mathbf{x}} = \nabla_{\mathbf{x}} A \cdot \tau_{\mathbf{x}} = 0$ , where  $\tau_{\mathbf{x}}$  is the tangential vector to  $\partial\Omega$  at  $\mathbf{x}$ . Hence since

$$\mathbf{U}_s \cdot \nu_{\mathbf{x}} = 0, \quad \text{on } \mathbf{x} \in \partial\Omega,$$

293 the right hand side is also zero in that case. Finally a further integration on  $r_z$  shows  
294 that

$$295 \quad (36) \quad \frac{d}{dt} \int_{\Omega} \int_{r_z} \phi(F_s) dr_z d\mathbf{x} = 0$$

or

$$\int_{\Omega} \int_{p_z} \phi(F_s(t)) dr_z d\mathbf{x} = \int_{\Omega} \int_{\mathbb{R}} \phi(F_s(0)) dr_z d\mathbf{x}, \quad t \geq 0.$$

296 Notice that this result still holds true when  $\phi$  is only continuous. Taking  $\phi(F) = F$ , it  
297 ensures the conservation of mass,  $\phi(F_s) = \max(0, F_s)$  gives the non-negativity of the  
298 distribution function for nonnegative initial datum, while  $\phi(F_s) = F_s^p$  for  $1 \leq p < \infty$ ,  
299 it yields the conservation of  $L^p$  norm.

Now let us show the conservation of total energy. On the one hand, we multiply the equation on  $F_i$  by  $\mathcal{H}_i$  and the one on  $F_e$  by  $\mathcal{H}_e$ , it gives after a simple integration by part and using the appropriate boundary conditions (31) or (32),

$$\int_{\Omega \times \mathbb{R}} \mathcal{H}_i \partial_t F_i + \mathcal{H}_e \partial_t F_e d\mathbf{x} dr_z = 0.$$

300 or

$$301 \quad (37) \quad \int_{\Omega \times \mathbb{R}} \frac{(A - r_z)^2}{2} \partial_t F_i + \frac{(A + r_z)^2}{2\alpha} \partial_t F_e d\mathbf{x} dr_z + \int_{\Omega \times \mathbb{R}} \partial_t (n_i - n_e) \Phi d\mathbf{x} = 0.$$

The first and second terms in the latter equality can be written as

$$\left\{ \begin{array}{l} \mathcal{I}_1 := \int_{\Omega \times \mathbb{R}} \frac{(A - r_z)^2}{2} \partial_t F_i d\mathbf{x} dr_z \\ \quad = \frac{d}{dt} \int_{\Omega \times \mathbb{R}} \frac{(A - r_z)^2}{2} F_i d\mathbf{x} dr_z - \int_{\Omega} (n_i A - n_i \mathbf{u}_i) \partial_t A d\mathbf{x} \\ \mathcal{I}_2 := \int_{\Omega \times \mathbb{R}} \frac{(A + r_z)^2}{2\alpha} \partial_t F_e d\mathbf{x} dr_z \\ \quad = \frac{d}{dt} \int_{\Omega \times \mathbb{R}} \frac{(A + r_z)^2}{2\alpha} F_e d\mathbf{x} dr_z - \frac{1}{\alpha} \int_{\Omega} (n_e A + n_e \mathbf{u}_e) \partial_t A d\mathbf{x}, \end{array} \right.$$

which yields using the equation on  $A$  in (15),

$$\mathcal{I}_1 + \mathcal{I}_2 = \frac{d}{dt} \int_{\Omega \times \mathbb{R}} \left[ \frac{(A - r_z)^2}{2} F_i + \frac{(A + r_z)^2}{2\alpha} F_e \right] d\mathbf{x} dr_z + \frac{1}{2\text{Ma}^2} \frac{d}{dt} \int_{\Omega} |\nabla_{\mathbf{x}} A|^2 d\mathbf{x}.$$

On the other hand, from the equation on  $\Phi$  in (15), we get

$$\mathcal{I}_3 := \int_{\Omega \times \mathbb{R}} \partial_t (n_i - n_e) \Phi d\mathbf{x} = \frac{1}{2} \frac{d}{dt} \int_{\Omega} |\nabla_{\mathbf{x}} \Phi|^2 d\mathbf{x}.$$

302 Finally, using that  $\mathcal{I}_1 + \mathcal{I}_2 + \mathcal{I}_3 = 0$  in (37), we obtain the energy conservation (35).  $\square$

303 From the conservation of moments (Proposition 2.6), we get  $L^p$  estimates [5] on  
304 the macroscopic quantities

LEMMA 2.7. *If  $F \in L^1 \cap L^\infty(\Omega \times \mathbb{R})$  and  $|r_z|^m F \in L^1(\Omega \times \mathbb{R})$  with  $0 \leq m < \infty$ , then we define*

$$n_F = \int_{\mathbb{R}} F dr_z, \quad n_{\mathbf{u}_F} = \int_{\mathbb{R}} F r_z dr_z, \quad e_F = \int_{\mathbb{R}} F |r_z|^2 dr_z$$

and there exists  $C > 0$  such that

$$\|n_F\|_{L^{1+m}} \leq C \|F\|_{L^\infty}^{m/(m+1)} \left( \int_{\Omega \times \mathbb{R}} |r_z|^m |F| dr_z d\mathbf{x} \right)^{1/(m+1)}$$

and

$$\begin{cases} \|n_{\mathbf{u}_F}\|_{L^{(1+m)/2}} \leq C \|F\|_{L^\infty}^{(m-1)/(m+1)} \left( \int_{\Omega \times \mathbb{R}} |r_z|^m |F| dr_z d\mathbf{x} \right)^{2/(m+1)}, \\ \|e_F\|_{L^{(1+m)/3}} \leq C \|F\|_{L^\infty}^{(m-2)/(m+1)} \left( \int_{\Omega \times \mathbb{R}} |r_z|^m |F| dr_z d\mathbf{x} \right)^{3/(m+1)}. \end{cases}$$

305 From Proposition 2.6 and Lemma 2.7 we can prove the existence of weak solutions to  
306 (15)

307 THEOREM 2.8 (Existence of weak solutions). *Assume that the nonnegative initial  
308 condition  $F_{s,\text{in}} \in L^1 \cap L^\infty(\Omega \times \mathbb{R})$  for  $s = i, e$  and for any  $m > 5$*

$$309 \quad (38) \quad \int_{\Omega \times \mathbb{R}} |r_z|^m F_s(0, \mathbf{x}, r_z) dr_z d\mathbf{x} < \infty.$$

310 *Then, there exists a weak solution  $(F_i, F_e, \Phi, A)$  to (15), with  $F_i, F_e \in L^\infty(\mathbb{R}^+, L^1 \cap$   
311  $L^\infty(\Omega \times \mathbb{R}))$ , and  $\Phi, A \in L^\infty(\mathbb{R}^+, W_0^{1,p}(\Omega))$ , for any  $p > 1$ .*

*Proof.* The proof follows the lines of the existence of weak solutions for the Vlasov-Poisson system [2, 13]. The main point here is to get enough compactness on the potential  $A$  since its equation is nonlinear

$$-\Delta_{\mathbf{x}} A + \text{Ma}^2 \left( n_i + \frac{n_e}{\alpha} \right) A = \text{Ma}^2 \mathcal{J}_z.$$

From (38) and Proposition 2.6, we first get the conservation of moments for any  $l \in (0, m]$  and  $s = i, e$

$$\int_{\Omega \times \mathbb{R}} |r_z|^l F_s(t) dr_z d\mathbf{x} = \int_{\Omega \times \mathbb{R}} |r_z|^l F_{s,\text{in}} dr_z d\mathbf{x} < \infty,$$

hence applying Lemma 2.7, it yields that for any  $r \in [1, m+1]$  and  $q \in [1, (m+1)/2]$

$$\rho = n_i - n_e \in L^\infty(\mathbb{R}^+, L^r(\Omega)), \quad \mathcal{J}_z \in L^\infty(\mathbb{R}^+, L^q(\Omega)).$$

Thus, from the elliptic equations in (15) for  $A$  and  $\Phi$ ,

$$\begin{cases} -\Delta_{\mathbf{x}}\Phi = \rho, \\ -\Delta_{\mathbf{x}}A + \text{Ma}^2 \left( n_i + \frac{n_e}{\alpha} \right) A = \text{Ma}^2 \mathcal{J}_z, \end{cases}$$

it yields

$$\nabla_{\mathbf{x}}\Phi \in L^\infty(\mathbb{R}^+, W_0^{1,r}(\Omega)), \quad \nabla_{\mathbf{x}}A \in L^\infty(\mathbb{R}^+, W_0^{1,q}(\Omega)).$$

312 Since we can choose  $r$  and  $q > 2$ , using classical Sobolev inequalities, we have in  
313 particular that both  $\nabla_{\mathbf{x}}\Phi$  and  $\nabla_{\mathbf{x}}A$  are uniformly bounded in  $L^\infty(\mathbb{R}^+ \times \Omega)$ .

Furthermore, we obtain an estimate on the time derivative  $\partial_t \nabla_{\mathbf{x}}\Phi$  and  $\partial_t \nabla_{\mathbf{x}}A$  by differentiating with respect to the two Poisson equations in (15)

$$\begin{cases} -\Delta_{\mathbf{x}}\partial_t\Phi = \partial_t\rho, \\ -\Delta_{\mathbf{x}}\partial_tA + \text{Ma}^2 \left( n_i + \frac{n_e}{\alpha} \right) \partial_tA = \text{Ma}^2 \partial_t\mathcal{J}_z - \text{Ma}^2 \left( \partial_t n_i + \frac{\partial_t n_e}{\alpha} \right) A. \end{cases}$$

Then using the evolution equation satisfied by  $\rho$  and  $\mathcal{J}_z$

$$\begin{cases} \partial_t\rho = \nabla_{\mathbf{x}} \cdot \left( \rho \nabla_{\mathbf{x}}^\perp \Phi + \left( n_i + \frac{n_e}{\alpha} \right) \frac{\nabla_{\mathbf{x}}^\perp A^2}{2} - \nabla_{\mathbf{x}}^\perp A \mathcal{J}_z \right), \\ \partial_t\mathcal{J}_z = \nabla_{\mathbf{x}} \cdot \left( \mathcal{J}_z \nabla_{\mathbf{x}}^\perp \Phi + \left( n_i \mathbf{u}_i + \frac{n_e \mathbf{u}_e}{\alpha^2} \right) \frac{\nabla_{\mathbf{x}}^\perp A^2}{2} - \nabla_{\mathbf{x}}^\perp A \left( e_i - \frac{e_e}{\alpha^2} \right) \right), \end{cases}$$

where  $e_s$  corresponds to the second order moment in  $r_z$ ,

$$e_s(t, \mathbf{x}) = \int_{\mathbb{R}} F_s(t) |r_z|^2 dr_z, \quad \text{for } s = i, e$$

314 and applying Lemma 2.7, we have that  $e_i, e_e \in L^\infty(\mathbb{R}^+, L^2(\Omega))$ , hence both terms  
315  $\partial_t \nabla_{\mathbf{x}}A$  and  $\partial_t \nabla_{\mathbf{x}}\Phi$  are uniformly bounded  $L^\infty(\mathbb{R}^+, L^2(\Omega))$ .

316 From these estimates, we get strong compactness on the electromagnetic field  
317  $\mathbf{E} = -\nabla_{\mathbf{x}}\Phi$  and  $\mathbf{B} = \nabla_{\mathbf{x}} \times A$  in  $L^2$  and weak compactness in  $L^2$  allowing to treat the  
318 nonlinear terms and prove existence of weak solutions for (15).  $\square$

319 **REMARK 2.9.** *Observing that starting from (15), and taking the limit  $\text{Ma} \rightarrow 0$ , it*  
320 *gives from the Poisson's equation that  $A = 0$ . Then we integrate (15) in  $r_z \in \mathbb{R}$  and*  
321 *we recover the two dimensional guiding-center model [21, 36, 29]*

$$322 \quad (39) \quad \begin{cases} \partial_t\rho + \nabla_{\mathbf{x}} \cdot (\mathbf{U}\rho) = 0, \\ -\Delta_{\mathbf{x}}\Phi = \rho, \end{cases}$$

323 with the divergence free velocity  $\mathbf{U} = -\nabla_{\mathbf{x}}^\perp \Phi$ .

324 **2.4. Guiding center model & linear instability.** To study the growth rate  
 325 of the linear instability for our asymptotic model (15), we follow the classical lin-  
 326 earization procedure: consider an equilibrium solution  $(F_{i,0}, F_{e,0}, \Phi_0, A_0)$  to (15) and  
 327 assume that

$$328 \quad (40) \quad \int_{\mathbb{R}} r_z F_{i,0} dr_z = \int_{\mathbb{R}} r_z F_{e,0} dr_z = 0.$$

329 Therefore the potential  $A_0$  satisfies a linear Poisson equation with a null source term  
 330 together with periodic boundary condition or zero Dirichlet boundary conditions,  
 331 which means that  $A_0 \equiv 0$ .

332 Now we consider  $(F_i, F_e, \Phi, A)$  a solution to the nonlinear system ((15)) and  
 333 decompose it as the sum of the equilibrium  $(F_{i,0}, F_{e,0}, \Phi_0, 0)$  and a perturbation  
 334  $(F'_i, F'_e, \Phi', A')$ ,

$$335 \quad F_i = F_{i,0} + F'_i, \quad F_e = F_{e,0} + F'_e, \quad \rho = \rho_0 + \rho', \quad \Phi = \Phi_0 + \Phi', \quad A = A'.$$

336 Then we substitute them into (15) and drop the high order small perturbation terms,  
 337 a linearized system is obtained as follows:

$$338 \quad (41) \quad \begin{cases} \partial_t F'_i - \nabla_{\mathbf{x}}^\perp \Phi_0 \cdot \nabla_{\mathbf{x}} F'_i - \nabla_{\mathbf{x}}^\perp (\Phi' - p_z A') \cdot \nabla_{\mathbf{x}} F_{i,0} = 0, \\ \partial_t F'_e - \nabla_{\mathbf{x}}^\perp \Phi_0 \cdot \nabla_{\mathbf{x}} F'_e - \nabla_{\mathbf{x}}^\perp \left( \Phi' - \frac{q_z}{\alpha} A' \right) \cdot \nabla_{\mathbf{x}} F_{e,0} = 0, \\ -\Delta_{\mathbf{x}} \Phi' = \rho', \\ -\Delta_{\mathbf{x}} A' + \text{Ma}^2 \left( n_{i,0} + \frac{n_{e,0}}{\alpha} \right) A' = \text{Ma}^2 \mathcal{J}'_z := \text{Ma}^2 \int_{\mathbb{R}} r_z \left( F'_i - \frac{F'_e}{\alpha} \right) dr_z. \end{cases}$$

339 Now we integrate the first equation in  $p_z \in \mathbb{R}$  and the second one in  $q_z \in \mathbb{R}$  and using  
 340 (40), we get a linearized system for the perturbed charge density

$$341 \quad (42) \quad \begin{cases} \partial_t \rho' - \nabla_{\mathbf{x}}^\perp \Phi_0 \cdot \nabla_{\mathbf{x}} \rho' - \nabla_{\mathbf{x}}^\perp \Phi' \cdot \nabla_{\mathbf{x}} \rho_0 = 0, \\ -\Delta_{\mathbf{x}} \Phi' = \rho', \end{cases}$$

342 which is exactly the linearized system for the two dimensional guiding-center model  
 343 (39).

344 Therefore, from an equilibrium  $(\rho_0, \Phi_0)$  for the guiding-center model (39), we can  
 345 easily construct an equilibrium for (15) by choosing  $F_{s,0}$  such that it satisfies (40) and

$$346 \quad (43) \quad \int_{\mathbb{R}} F_{s,0} dr_z = n_{s,0}, \quad \text{for } s = i, e.$$

where  $n_{s,0}$  is the equilibrium density satisfying  $\rho_0 = n_{i,0} - n_{e,0}$ . For instance, we can  
 choose

$$F_{s,0} = \frac{n_{s,0}}{\sqrt{2\pi}} \exp\left(-\frac{r_z^2}{2}\right).$$

347 In terms of the electric charge density  $\rho$  and potential  $\Phi$ , our asymptotic model  
 348 has the same mechanism for generating instabilities as the two dimensional guiding-  
 349 center model, so that the growth rate of instabilities for the electric field will be the  
 350 same. We can refer to [33, 29, 11] for the analytical and numerical studies of the two

351 dimensional guiding-center model. In the next section, we will numerically verify that  
 352 the linear growth rates of instabilities for the electric potential of the two models are  
 353 the same.

354 From this point, we observe that by choosing a nonzero initial potential  $A$ , that  
 355 is a small current density  $\mathcal{J}_z$ , we can initiate an instability on the asymptotic model  
 356 (15), whereas the purely electrostatic guiding center model remains stationary.

357 **REMARK 2.10.** *We would notice that for the distribution function  $F_i$  or  $F_e$ , due to*  
 358 *the extra term of  $\nabla_{\mathbf{x}}^\perp(p_z A') \cdot \nabla_{\mathbf{x}} F_{i,0}$  and  $\nabla_{\mathbf{x}}^\perp(q_z A'/\alpha) \cdot \nabla_{\mathbf{x}} F_{e,0}$  in the first two equations*  
 359 *of (41), some other instabilities might also happen to  $F'_i$  or  $F'_e$ , which is much more*  
 360 *complicated to analyze.*

361 **3. Numerical Examples.** In this section, we will perform numerical tests for  
 362 the diocotron instability and the Kelvin-Helmholtz instability problems to illustrate  
 363 some good properties of the asymptotic kinetic model (15) involving a self-consistent  
 364 electromagnetic field, and compare with the macroscopic guiding-center model (39)  
 365 taking into account only electrostatic effects [36, 29]. We will apply a conservative  
 366 finite difference scheme with Hermite weighted essentially non-oscillatory (WENO) re-  
 367 construction, coupled with a fourth-order Runge-Kutta time discretization for solving  
 368 the conservative transport equations. The Poisson's equation for the electric poten-  
 369 tial function  $\Phi$  will be solved by a 5-point central finite difference discretization for  
 370 Dirichlet boundary conditions, or by the fast Fourier transform (FFT) for periodic  
 371 boundary conditions on a rectangular domain. The elliptic equation for the magnetic  
 372 potential  $A$  is solved by a 5-point central finite difference discretization. The methods  
 373 are natural extensions of those proposed in [36] for solving the guiding-center model  
 374 (39), since here the velocity field  $p_z$  or  $q_z$  in the transport equations only appears as a  
 375 dummy argument. A mid-point rule with spectral accuracy [6] is used for the moment  
 376 integration. We omit the description of these methods and refer to [36] for details.

377 We mainly show that the asymptotic model (15) can generate the same instability  
 378 as the two dimensional guiding-center model (39), while some other instabilities can  
 379 also be created due to some small perturbations purely in the self-consistent magnetic  
 380 field. In the following, for the asymptotic kinetic model (15), we all take the cut-off  
 381 domain in velocity as  $[-8, 8]$  and discretize it with  $N = 32$  uniform grid points.

**3.1. Diocotron instability.** We set

$$\mathcal{H} = \Phi + \frac{1}{2}(A - p_z)^2$$

382 and consider the nonlinear asymptotic model (15) where the density of electrons is  
 383 neglected and the reduced distribution function of ions is denoted by  $F$  and is a  
 384 solution to

$$385 \quad (44) \quad \begin{cases} \partial_t F - \nabla_{\mathbf{x}}^\perp \mathcal{H} \cdot \nabla_{\mathbf{x}} F = 0, \\ -\Delta \Phi = n, \\ -\Delta A + \text{Ma}^2 n A = \text{Ma}^2 \mathcal{J}_z, \end{cases}$$

where

$$n = \int_{\mathbb{R}} F(t) dp_z, \quad \mathcal{J}_z = \int_{\mathbb{R}} F(t) p_z dp_z.$$

386 This solution can be compared to the two dimensional guiding center model (39),  
 387 where we neglect the effect of the self-consistent magnetic field  $\mathbf{B} = \nabla_{\mathbf{x}} \times A$ , corre-  
 388 sponding to the low Mach number limit  $\text{Ma} \rightarrow 0$  of (44), it yields

$$389 \quad (45) \quad \begin{cases} \partial_t n - \nabla_{\mathbf{x}}^\perp \Phi \cdot \nabla_{\mathbf{x}} n = 0, \\ -\Delta \Phi = n. \end{cases}$$

390 In this example, we choose  $\text{Ma} = 0.1$  and we would like to verify that the asymp-  
 391 totic kinetic model (44) has indeed the same instability on the density  $n$  as compared  
 392 to the two dimensional guiding-center model (45). We choose a discontinuous initial  
 393 density  $n_0$  which is linearly unstable [11, 29]. Therefore, we consider  $\Omega$  as a ball  
 394 centered in 0 of radius  $R = 10$  with the initial density

$$395 \quad (46) \quad n_0(\mathbf{x}) = \begin{cases} 1 + \varepsilon \cos(l\theta), & \text{if } r^- \leq \sqrt{x^2 + y^2} \leq r^+, \\ 0, & \text{else,} \end{cases}$$

396 where  $\varepsilon = 0.02$ ,  $l = 3$ ,  $r^- = 3$ ,  $r^+ = 5$ , which will create a small instability for the  
 397 two-dimensional model (45).

398 Now for the asymptotic model (44), we still consider the same density  $n_0$  as an  
 399 initial data, but introduce an additional perturbation on the moment  $p_z$  by choosing

$$400 \quad (47) \quad F_0(\mathbf{x}, p_z) = \frac{n_0(\mathbf{x})}{\sqrt{2\pi}} \exp\left(-\frac{(p_z - u_0(\mathbf{x}))^2}{2}\right).$$

401 with  $u_0 = \delta \cos(m\theta)$ , where  $\theta = \text{atan2}(y, x)$ ,  $\delta = 0.1$ ,  $m = 3$ . It is expected that the  
 402 instability will now be driven by the perturbation on the density  $n_0$  corresponding  
 403 to the mode  $l = 3$  but also by the perturbation on the current density  $\mathcal{J}_z$  due to  $u_0$   
 404 corresponding to the mode  $m = 3$ .

405 In Figure 1, we can clearly see three vortexes are formed at  $t = 40$ , which is  
 406 the same as the diocotron instability for the two dimensional guiding-center model  
 407 (45) and agrees with the linear instability analysis in Section 2.4. At  $t = 60, 80, 100$ ,  
 408 these vortexes continue moving and start to mix with each other. Here the grid is  
 409  $N_x \times N_y = 600 \times 600$ . However, we would notice that for the current density  $\mathcal{J}_z$ ,  
 410 as shown in Figure 2, we can also observe three vortexes, which might be caused by  
 411 the perturbation on the moment  $p_z$  from the self-consistent magnetic field which are  
 412 different from the instabilities of the density  $n$ .

413 In Figure 3, we show the time evolution of the  $L^\infty$  norm for the difference of the  
 414 electrical potential  $\|\Phi(t) - \Phi(0)\|_{L^\infty}$  and  $\|A(t)\|_{L^\infty}$ , on the grids of  $N_x \times N_y = 600 \times 600$   
 415 and  $N_x \times N_y = 300 \times 300$ . We can see convergent results. Especially an exponential  
 416 growth rate on  $\|\Phi(t) - \Phi(0)\|_{L^\infty}$  can be observed for  $t < 50$ , while the magnitude of  
 417 the self-consistent magnetic field  $A$  is at the level of  $10^{-4}$ . We measure the growth  
 418 rate for  $\|\Phi(t) - \Phi(0)\|_{L^\infty}$  by taking the time interval  $[10, 30]$ , so the growth rate is  
 419 about 0.0999. The growth rate from a linear instability analysis based on the formula  
 420 (6.38)-(6.42) in [11] with  $\omega_D = 1/2$ , is about 0.1051. These two growth rates agree  
 421 with each other very well.

422 We also note that for this example, the dominating instability would be caused  
 423 by the perturbation on the initial density  $n_0$ . Numerically we observe the exponential  
 424 growth rate of  $\|\Phi(t) - \Phi(0)\|_{L^\infty}$  for the two dimensional guiding center model is almost  
 425 the same as the asymptotic model and we omit them in Figure 3 for clarity.

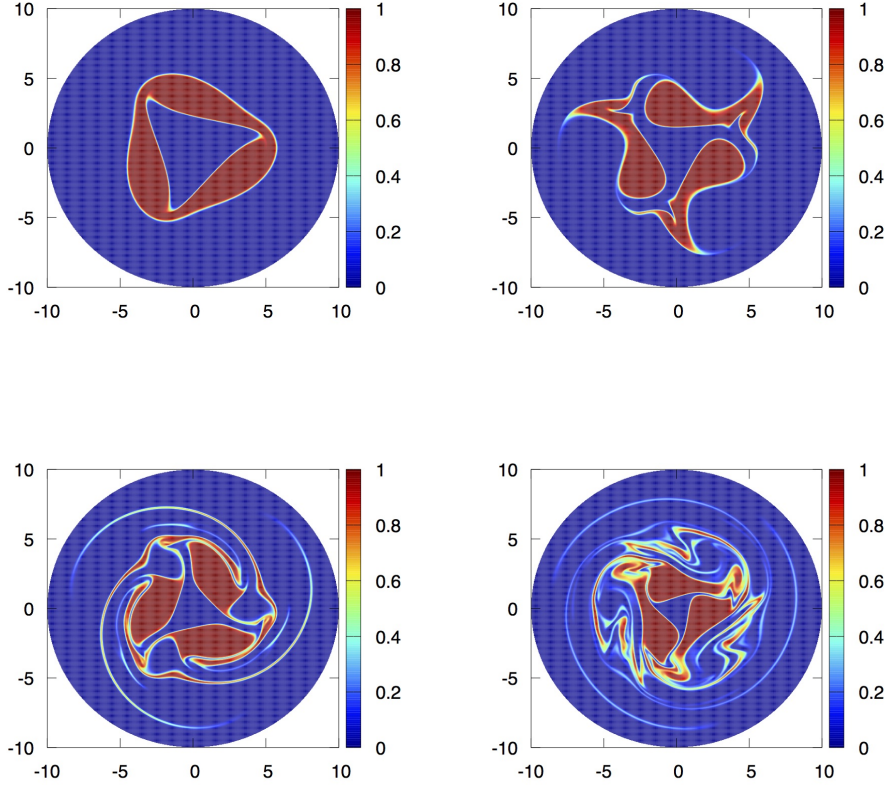


FIG. 1. **Diocotron instability.** The density  $n$  for the  $2d \times 1d$  asymptotic model (15). From left to right, top to bottom:  $t = 40, 60, 80, 100$ .

426 The time evolutions of the relative difference for the total energy (35) and the  $L^2$   
 427 norm of  $F$  are preserved relatively well for this example, which are at the loss of 0.2%  
 428 and 25% up to  $t = 150$  respectively, on the grid of  $N_x \times N_y = 600 \times 600$ , especially  
 429 the total energy can be greatly improved by mesh refinement. We omit the figures  
 430 here to save space.

431  
 432  
 433

434 **3.2. Kelvin-Helmholtz instability.** In this example, we consider a plasma for  
 435 ions with a neutral background. The distribution function  $F$  of the asymptotic model

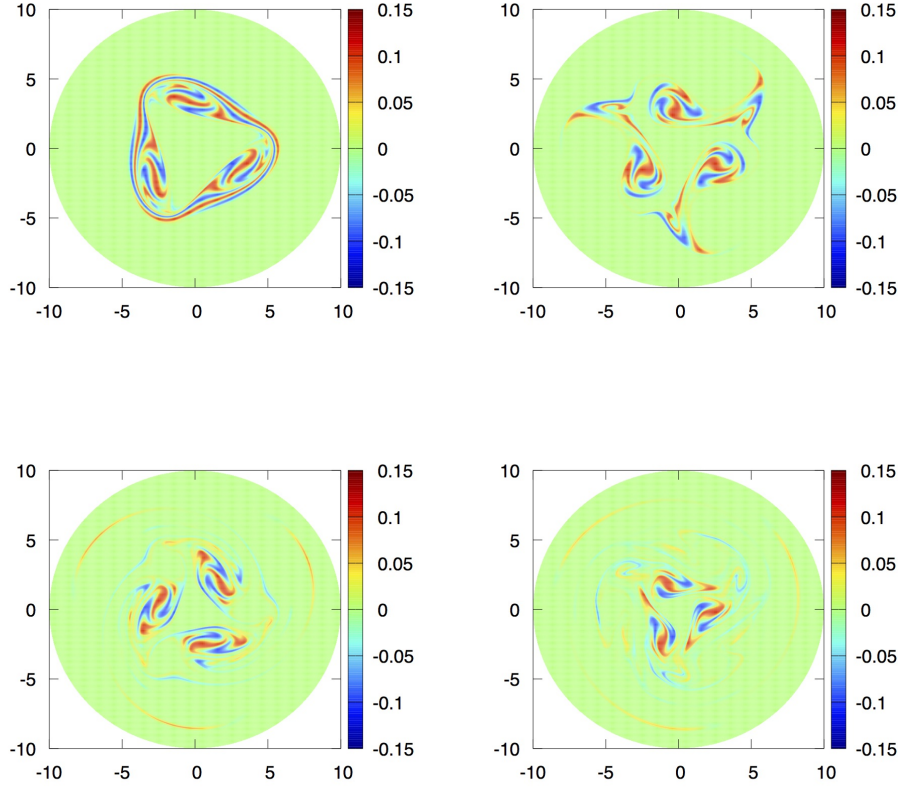


FIG. 2. **Diocotron instability.** The current density  $\mathcal{J}_z$  for the  $2d \times 1d$  asymptotic model (15). From left to right, top to bottom:  $t = 40, 60, 80, 100$ .

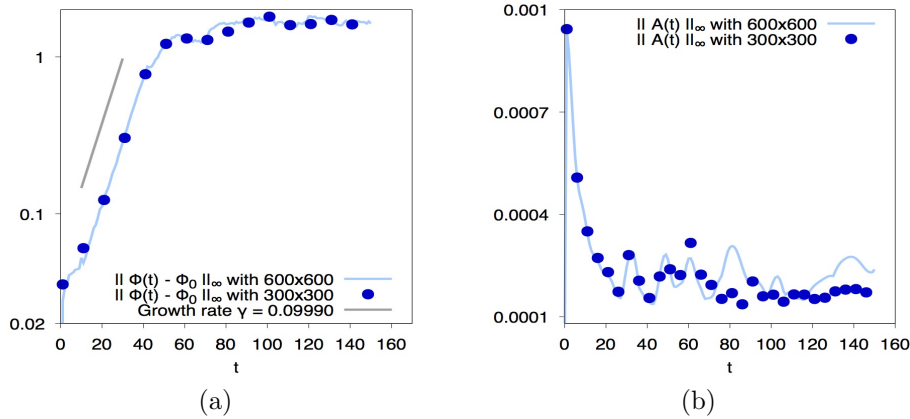


FIG. 3. **Diocotron instability.** Time evolution of the norm  $\|\Phi(t) - \Phi(0)\|_{L^\infty}$  and  $\|A(t) - A(0)\|_{L^\infty}$  for the  $2d \times 1d$  asymptotic model (15).

436 (44) for the ions is a solution to the following system

$$437 \quad (48) \quad \begin{cases} \partial_t F - \nabla_{\mathbf{x}}^\perp \left( \Phi + \frac{A^2}{2} - p_z A \right) \cdot \nabla_{\mathbf{x}} F = 0, \\ -\Delta_{\mathbf{x}} \Phi = \rho := n - n_e, \\ -\Delta_{\mathbf{x}} A + \text{Ma}^2 \left( n + \frac{n_e}{\alpha} \right) A = \text{Ma}^2 \mathcal{J}_z, \end{cases}$$

with  $\alpha = 1/1836.5$  which corresponds to the mass ratio of one electron and one proton. The current density is

$$\mathcal{J}_z = \int_{\mathbb{R}} F(t) p_z dp_z$$

438 and we choose the initial density  $n$  for the ions to be

$$439 \quad (49) \quad n_0(\mathbf{x}) = 2 + \sin y,$$

440 while for the electrons, we fix it with  $n_e = 2$  so that the spatial average is 0 for the  
441 total charge density  $\rho = n - n_e$ . We take the initial distribution function  $F$  of the  
442 ions as

$$443 \quad (50) \quad F_0(\mathbf{x}, p_z) = \frac{n_0(\mathbf{x})}{\sqrt{2\pi}} \exp\left(-\frac{(p_z - u_0(\mathbf{x}))^2}{2}\right),$$

444 where the shifted velocity  $u_0(\mathbf{x})$  is

$$445 \quad (51) \quad u_0(\mathbf{x}) = -0.01 \left( \sin\left(\frac{x}{2}\right) - \cos(y) \right),$$

which contributes as a small perturbation in the  $p_z$  direction and its corresponding  
initial current density  $\mathcal{J}_z$  will be small but nonzero. The distribution function of the  
electrons  $F_e$  is set to be at an equilibrium as

$$F_e := F_e(q_z) = \frac{n_e}{\sqrt{2\pi}} \exp\left(-\frac{q_z^2}{2}\right),$$

446 so that  $\int_{\mathbb{R}} F_e(r_z) r_z dr_z = 0$  and it does not contribute to the total current  $\mathcal{J}_z$  in the  
447 equation of (17) for the magnetic potential  $A$ . Similarly if we neglect the effect of the  
448 self-consistent magnetic field  $\mathbf{B}$ , which corresponds to the low Mach limit  $\text{Ma} \rightarrow 0$  of  
449 (48), it yields the two-dimensional guiding center model in the following form

$$450 \quad (52) \quad \begin{cases} \partial_t n - \nabla_{\mathbf{x}}^\perp \Phi \cdot \nabla_{\mathbf{x}} n = 0, \\ -\Delta \Phi = n - n_e. \end{cases}$$

451 The computational domain is on a square  $[0, 4\pi] \times [0, 2\pi]$  with periodic boundary  
452 conditions and the Mach number in (48) is taken to be  $\text{Ma} = 0.1$ .

453 Here we see that without perturbation on the initial data (49), the density  $n$  of  
454 the  $2d$  guiding-center model (52) is at the steady state  $n(t, \mathbf{x}) = \sin(y)$ . Furthermore,  
455 when we choose  $u_0 \equiv 0$ , the solution is at steady state for both models (52) and (48)  
456 and remains stable on the time interval  $[0, 100]$ . However, for the asymptotic model  
457 (48) with a non zero  $u_0$  as (51), due to the effect of the self-consistent magnetic field

458  $A$  and a small nonzero current  $\mathcal{J}_z$ , we observe in Figure 4 that some instabilities are  
 459 created on the density  $n$  at  $t = 40, 60, 80, 100$ . Here the grid is  $N_x \times N_y = 256 \times 256$ .  
 460 These instabilities are very similar to the Kelvin-Helmholtz instability for the  $2d$   
 461 guiding-center model (52) as compared to Figure 9 in [18], which do not happen on  
 462 the current settings. Moreover, these instability structures can also be observed on  
 463 the current density  $\mathcal{J}_z$  as shown in Figure 5, which greatly indicate the capability of  
 464 the self-consistent magnetic field as another source on the development of physical  
 465 instabilities.

466 For the  $2d \times 1d$  asymptotic model, in Figure 6 we show the time evolution of the  
 467  $L^\infty$  norm for the difference of the electrical potential  $\|\Phi(t) - \Phi(0)\|_{L^\infty}$  and  $\|A(t)\|_{L^\infty}$ ,  
 468 on the grids of  $N_x \times N_y = 256 \times 256$  and  $N_x \times N_y = 128 \times 128$ . The results are also  
 469 convergent and an exponential growth rate is observed for  $\|\Phi(t) - \Phi(0)\|_{L^\infty}$  for  $t < 65$ ,  
 470 which explicitly demonstrates the instabilities caused by the small current density  $\mathcal{J}_z$   
 471 on the self-consistent magnetic field  $A$ , even we notice that the magnitude of  $A$  is  
 472 overall getting smaller as shown on the right side of Figure 6. Here we are also able to  
 473 measure the growth rate for  $\|\Phi(t) - \Phi(0)\|_{L^\infty}$  by taking the time interval  $[20, 40]$ , the  
 474 growth rate is about 0.2606, which is very close to the growth rate from the numerical  
 475 predicted value 0.26 in [33] (see Figure 1 with  $k_y = 0.5$  and  $k_{ys} = 1$ ) for the two  
 476 dimensional nonlinear guiding-center model, which indicates that the instability for  
 477 these two models might be similar.

478 Similar to the last example, the time evolutions of the relative difference for the  
 479 total energy (35) and the  $L^2$  norm of  $F$  are preserved well, which are only at the loss  
 480 of 0.2% and 2.5% respectively, up to  $t = 100$  on the grid of  $N_x \times N_y = 256 \times 256$ . We  
 481 also omit the figures here.

482

483

484

485 **4. Conclusion.** In this paper, an asymptotic kinetic model is derived from a  $2d \times$   
 486  $3d$  Vlasov-Maxwell system, by taking into account of the self-consistent magnetic field.  
 487 We have assumed both a large applied magnetic field and large time in the asymptotic  
 488 limit. The new asymptotic model could validate some effect on the dynamics of the  
 489 plasma from the self-consistent magnetic field, even if initially the current is small, as  
 490 compared to the two dimensional guiding-center model for the Vlasov-Poisson system.  
 491 Numerical examples demonstrate the good properties of our new model.

492 **Acknowledgement.** Francis Filbet and Eric Sonnendrücker were supported by  
 493 the EUROfusion Consortium and has received funding from the Euratom research  
 494 and training programme 2014-2018 under grant agreement No 633053. The views and  
 495 opinions expressed herein do not necessarily reflect those of the European Commission.

496 T. Xiong acknowledges support from the Marie Skłodowska-Curie Individual Fel-  
 497 lowships H2020-MSCA-IF-2014 of the European Commission, under the project HN-  
 498 SKMAP 654175. This work has also been supported by the Fundamental Research  
 499 Funds for the Central Universities No. 20720160009 and National Natural Science  
 500 Foundation of China (NSFC) under grants 11601455, U1630247.

501

## REFERENCES

502 [1] T. M. ANTONSEN AND B. LANE, *Kinetic equations for low frequency instabilities in inhomoge-*  
 503 *neous plasmas*, Phys. Fluids, 23 (1980), pp. 1205–1214.

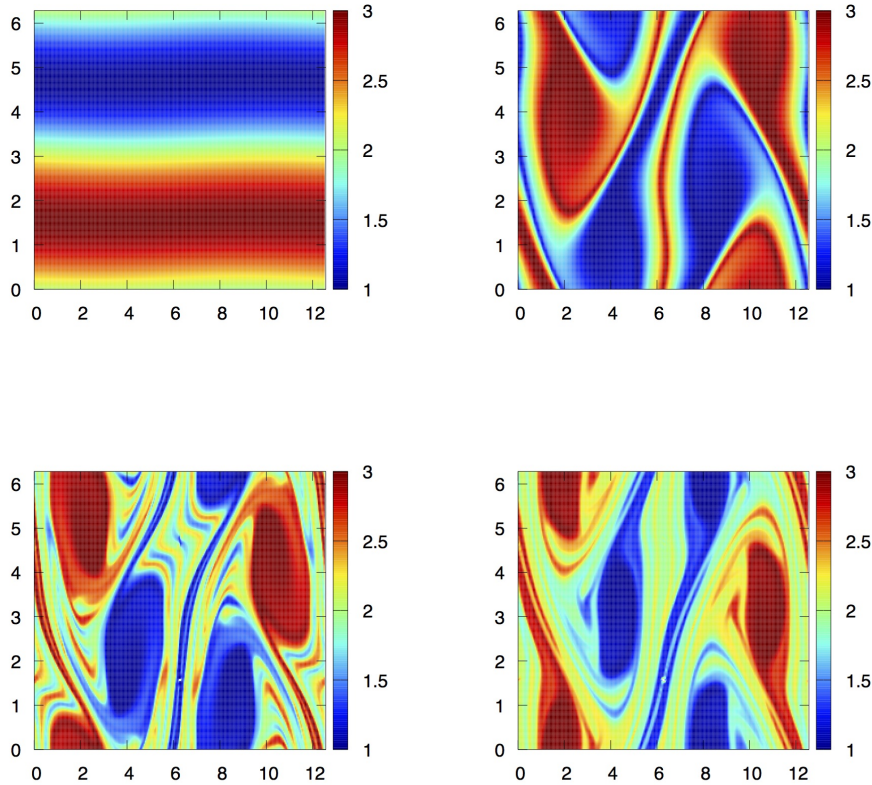


FIG. 4. **Kelvin-Helmholtz instability.** The density  $n$  for the  $2d \times 1d$  asymptotic model (48). From left to right, top to bottom:  $t = 40, 60, 80, 100$ .

- 504 [2] A. A. ARSEN'EV, *Existence in the large of a weak solution of Vlasov's system of equations*, *Ž.*  
 505 *Vyčisl. Mat. i Mat. Fiz.*, 15 (1975), pp. 136–147, 276.
- 506 [3] P. BELLAN, *Fundamentals of Plasma Physics*, Cambridge University Press, (2006).
- 507 [4] M. BOSTAN, *The Vlasov-Poisson system with strong external magnetic field. Finite Larmor*  
 508 *radius regime*, *Asymptot. Anal.*, 61 (2009), pp. 91–123.
- 509 [5] F. BOUCHUT, F. GOLSE, AND M. PULVIRENTI, *Kinetic equations and asymptotic theory*, B.  
 510 Perthame et L. Desvillettes eds, Series in Applied Mathematics, 4 (2000).
- 511 [6] J. P. BOYD, *Chebyshev and Fourier spectral methods*, Courier Dover Publications, 2001.
- 512 [7] Y. BRENIER, *Convergence of the Vlasov-Poisson system to the incompressible Euler equations*,  
 513 *Comm. in Partial Differential Equations*, 25 (2000), pp. 737–754.
- 514 [8] A. J. BRIZARD AND T. S. HAH, *Foundations of Nonlinear Gyrokinetic Theory*, *Rev. Modern*  
 515 *Phys.*, 79 (2007), pp. 421–468.
- 516 [9] N. CROUSEILLES, M. LEMOU, AND F. MÉHATS, *Asymptotic Preserving schemes for highly os-*  
 517 *cillatory Vlasov-Poisson equations*, *J. Comput. Phys.*, 248 (2013), pp. 287–308.
- 518 [10] N. CROUSEILLES, M. MEHRENBARGER, AND E. SONNENDRÜCKER, *Conservative semi-Lagrangian*  
 519 *schemes for Vlasov equations*, *J. Comput. Phys.*, 229 (2010), pp. 1927–1953.
- 520 [11] R. C. DAVIDSON, *Physics of nonneutral plasmas*, Imperial College Press London, 2001.
- 521 [12] P. DEGOND AND F. FILBET, *On the asymptotic limit of the three dimensional Vlasov-Poisson*  
 522 *system for large magnetic field: formal derivation*, arXiv preprint arXiv:1603.03666,  
 523 (2016).
- 524 [13] R. DI PERNA AND P.-L. LIONS, *Solutions globales d'équations du type Vlasov-Poisson*, C. R.

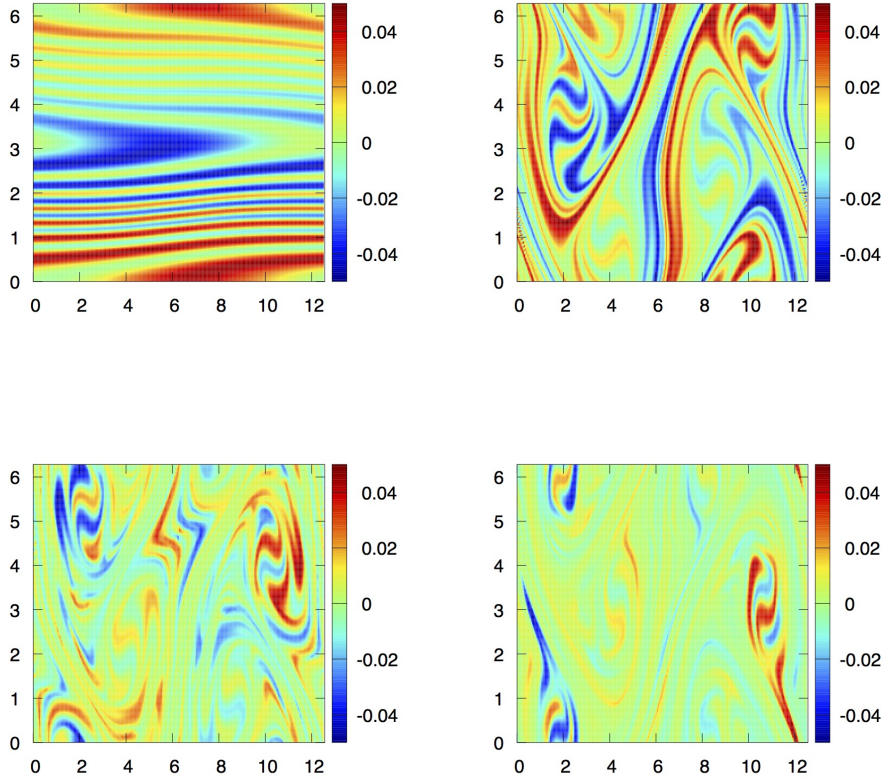


FIG. 5. **Kelvin-Helmholtz instability.** The current density  $J_z$  for the  $2d \times 1d$  asymptotic model (48). From left to right, top to bottom:  $t = 40, 60, 80, 100$ .

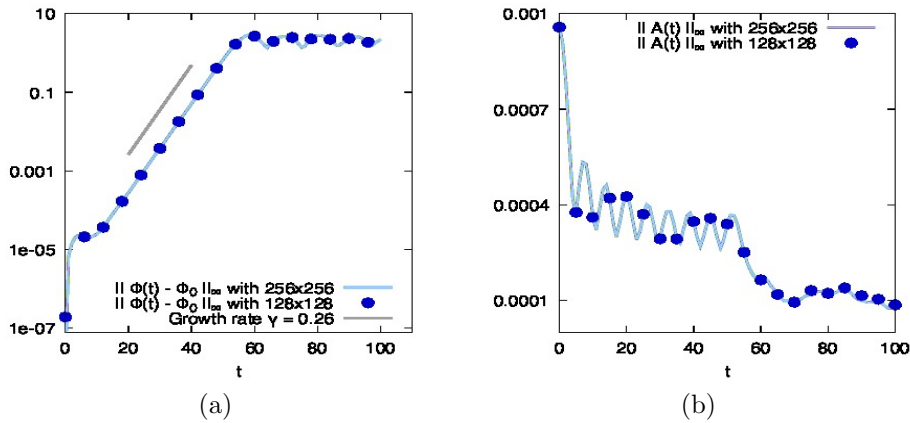


FIG. 6. **Kelvin-Helmholtz instability.** Time evolution of the norm  $\|\Phi(t) - \Phi(0)\|_{L^\infty}$  and  $\|A(t) - A(0)\|_{L^\infty}$  for the  $2d \times 1d$  asymptotic model (48).

- 525 Acad. Sci. Paris Sér. I Math., 307 (1988), pp. 655–658.
- 526 [14] P.-A. R. E. FRÉNO D AND E. SONNENDRÜCKER, *Two-scale expansion of a singularly perturbed*  
527 *convection equation*, J. Math. Pures Appl., 80 (2001), pp. 815–843.
- 528 [15] F. FILBET, *Convergence of a finite volume scheme for the Vlasov-Poisson system*, SIAM J.  
529 Numer. Anal., 39 (2001), pp. 1146–1169.
- 530 [16] F. FILBET AND L. M. RODRIGUES, *Asymptotically stable particle-in-cell methods for the Vlasov-*  
531 *Poisson system with a strong external magnetic field*, SIAM J. Numer. Anal., 54 (2016),  
532 pp. 1120–1146.
- 533 [17] F. FILBET AND C. YANG, *An inverse Lax-Wendroff method for boundary conditions applied to*  
534 *Boltzmann type models*, J. Comput. Phys., 245 (2013), pp. 43–61.
- 535 [18] E. FRÉNO D, S. A. HIRSTOAGA, M. LUTZ, AND E. SONNENDRÜCKER, *Long time behaviour of an*  
536 *exponential integrator for a Vlasov-Poisson system with strong magnetic field*, Commun.  
537 Comput. Phys., 18 (2015), pp. 263–296.
- 538 [19] E. FRÉNO D AND E. SONNENDRÜCKER, *Homogenization of the Vlasov equation and of the Vlasov-*  
539 *Poisson system with a strong external magnetic field*, Asymptot. Anal., 18 (1998), pp. 193–  
540 213.
- 541 [20] E. FRÉNO D AND E. SONNENDRÜCKER, *Long time behavior of the two-dimensional Vlasov equa-*  
542 *tion with a strong external magnetic field*, Math. Models Methods Appl. Sci., 10 (2000),  
543 pp. 539–553.
- 544 [21] F. GOLSE AND L. SAINT-RAYMOND, *The Vlasov-Poisson system with strong magnetic field*, J.  
545 Maths. Pures Appl., 78 (1999), pp. 791–817.
- 546 [22] F. GOLSE AND L. SAINT-RAYMOND, *The Vlasov-Poisson system with strong magnetic field in*  
547 *quasineutral regime*, Math. Models Methods Appl. Sci, 13 (2003), pp. 661–714.
- 548 [23] D. HAN-KWAN, *The three-dimensional finite larmor radius approximation*, Asymptot. Anal.,  
549 66 (2010), pp. 9–33.
- 550 [24] D. HAN-KWAN, *Effect of the polarization drift in a strongly magnetized plasma*, ESAIM Math.  
551 Model. Numer. Anal., 46 (2012), pp. 929–947.
- 552 [25] D. HAN-KWAN, *On the three-dimensional finite larmor radius approximation: the case of elec-*  
553 *trons in a fixed background of ions*, Ann. Inst. H. Poincaré Anal. Non Linear, 30 (2013),  
554 pp. 1127–1157.
- 555 [26] M. HAURAY AND A. NOURI, *Well-posedness of a diffusive gyro-kinetic model*, Ann. Inst. H.  
556 Poincaré Anal. Non Linear, 28 (2011), pp. 529–550.
- 557 [27] R. D. HAZELTINE AND J. D. MEISS, *Plasma Confinement*, Dover Publications, Mineola, New  
558 York, (2003).
- 559 [28] R. D. HAZELTINE AND A. A. WARE, *The drift kinetic equation for toroidal plasmas with large*  
560 *mass velocities*, Plasma Phys., 20 (1978), pp. 673–678.
- 561 [29] E. MADAULE, S. A. HIRSTOAGA, M. MEHRENBARGER, AND J. PÉTRI, *Semi-Lagrangian simula-*  
562 *tions of the diocotron instability*, Research Report, (2013).
- 563 [30] K. MIYAMOTO, *Plasma Physics and Controlled Nuclear Fusion*, Cambridge University Press,  
564 (2006).
- 565 [31] M. H. PH. GHENDRIH AND A. NOURI, *Derivation of a gyrokinetic model. existence and unique-*  
566 *ness of specific stationary solution*, Kinet. Relat. Models, 2 (2009), pp. 707–725.
- 567 [32] L. SAINT-RAYMOND, *Control of large velocities in the two-dimensional gyrokinetic approxima-*  
568 *tion*, J. Math. Pures Appl., 81 (2002), pp. 379–399.
- 569 [33] M. M. SHOUCRI, *A two-level implicit scheme for the numerical solution of the linearized vor-*  
570 *ticity equation*, International Journal for Numerical Methods in Engineering, 17 (1981),  
571 pp. 1525–1538.
- 572 [34] E. SONNENDRÜCKER, F. FILBET, A. FRIEDMAN, E. OUDET, AND J. VAY, *Vlasov simulations of*  
573 *beams with a moving grid*, Computer Physics Communications, 164 (2004), pp. 390–395.
- 574 [35] T. XIONG, G. RUSSO, AND J.-M. QIU, *Conservative multi-dimensional semi-Lagrangian finite*  
575 *difference scheme: Stability and applications to the kinetic and fluid simulations*, arXiv  
576 preprint arXiv:1607.07409, (2016).
- 577 [36] C. YANG AND F. FILBET, *Conservative and non-conservative methods based on Hermite*  
578 *weighted essentially non-oscillatory reconstruction for Vlasov equations*, J. Comput. Phys.,  
579 279 (2014), pp. 18–36.